



UNIVERSITA' POLITECNICA DELLE MARCHE

FACOLTA' DI INGEGNERIA

Master's Degree in Biomedical Engineering

Curriculum: Medical Devices

**Enhancing Osseointegration of Titanium Implants
with Heterologous Decellularized Bone
Grafts: Chimerization Strategies and In Vitro
Evaluation**

Supervisor:

Prof. Lorenzo Scalise

Co-Supervisor:

Paolo Fattori

Candidate:

Sara Falghera

Academic Year: 2022/2023

SUMMARY

ABSTRACT	1
INTRODUCTION.....	2
1. TITANIUM AND TITANIUM-ALLOYS.....	2
1.2. TITANIUM PROSTHESIS.....	4
1.2.1. ORTHOPEDIC IMPLANTS AND TITANIUM ORTHOPEDIC IMPLANTS	6
1.2.2. NEUROSURGERY IMPLANTS AND TITANIUM NEUROSURGERY IMPLANTS	7
2. CURRENT TITANIUM INTEGRATION TECHNOLOGIES	9
3. OSSEOINTEGRATION FAILURE	11
4. IMPLANT COATING TECHNIQUES.....	14
4.1. PHYSICAL DEPOSITION METHODS.....	15
4.2. CHEMICAL DEPOSITION METHODS	18
4.3. CHIMERA COATING	22
5. COATING MATERIALS.....	23
6. ANALYTIC TECHNIQUES	25
6.1. SDS PAGE	25
6.2. IR Spectroscopy	27
MATERIALS AND METHODS.....	29
1. REAGENTS AND DEVICES	32
2. GENERAL PROCEDURE	36
2.1. 1ST° TEST.....	37
2.2. 2ND° TEST.....	37
2.3. 3RD° TEST.....	38
2.4. 4TH° TEST.....	38
2.5. 5TH° TEST.....	39
2.6. 6TH° TEST.....	40
2.7. 7TH° TEST.....	40
2.8. 8TH° TEST.....	41
2.9. 9TH° TEST.....	42
2.10. 10TH° TEST.....	43
2.11. 11TH° TEST.....	43
2.12. 12TH° TEST.....	44
2.13. 13TH° TEST.....	44
2.14. 14TH° TEST.....	45
2.15. 15TH° TEST.....	46
2.16. 16TH° TEST.....	46

2.17. 17TH° TEST	47
3. IR-SPECTROSCOPY	49
3.2. PROTOCOL OF ANALYSIS	51
4. SDS PAGE.....	52
RESULTS.....	57
1. SURFACE INSPECTION	57
2. IR- ANALYSIS.....	64
3. SDS PAGE.....	66
DISCUSSIONS	68
CONCLUSIONS.....	71
REFERENCES.....	72

List of Figures

Figure 1 Crystal structure of hcp α and bcc β phase [4].....	3
Figure 2 (A) Total hip and (B) Knee Replacement [10]	7
Figure 3 (A) Plates, (B) Screws, (C) Radiographic scan of implanted pins, (D) Radiographic scan of wire, (E) Intramedullary rods [10].....	7
Figure 4 Titanium cranioplasty kit: (a) Titanium plate, (b)Titanium mesh [48].....	9
Figure 5 Spinal fixation devices[49]	9
Figure 6 Examples of Implant Failure [50].....	12
Figure 7 Mode 1 is the only wear mode associated with joint articulation, it occurs at the intended bearing surfaces (femoral head and acetabular cup). Modes 2, 3 and 4 occur at other nonintentional articulations as a function of prosthesis materials, design and implementation mode. [51]	13
Figure 8 Periprosthetic fracture [52]	14
Figure 9 Plasma Spray equipment [53].....	16
Figure 10 PLD equipment [54]	17
Figure 11 CVD equipment [55]	19
Figure 12 Sol-Gel process [56]	20
Figure 13 Stages of the Dip Coating process [21]	21
Figure 14 Spin Coating process [57].....	22
Figure 15 SDS-PAGE equipment [41].....	26
Figure 16 IR SPECTROSCOPY system [58]	28
Figure 17 In the left picture there is the reactor, in the right one there is the oven	30
Figure 18 RETSCH SK 300 on the left and on the right.....	31
Figure 19 RETSCH ZM 200	32
Figure 20 Grade 6 titanium bar (on the top), Grade 4 titanium screw (on the bottom)	33
Figure 21 Some of the reagents used	34
Figure 22 Scout™ STX1202 (left); Adventurer™ Analytical AX124 (right).....	35
Figure 23 M3-D Magnetic stirrer with ceramic heating plate (left); Ultrasonic cleaner DK-80 (right).....	35
Figure 24 PURELAB® Flex 3 water dispenser and deionization system	36
Figure 25 ZEISS Stemi 508 (left) and Axiocam ERc 5s (right)	36
Figure 26 Schematic representation of passages common to all tests.....	37
Figure 27 Principle of UATR operation [61]	50
Figure 28 Spectrum Two FT-IR with Universal ATR Accessory [62].....	50
Figure 29 Spectrum 10 Software Suite (PerkinElmer).....	51
Figure 30 Schematic representation of the IR-analysis protocol	52
Figure 31 Test tubes with P and M samples ready to be placed in the shaker.....	53
Figure 32 Sample M: A and B in the row above and Sample M: A and B in the row below ..	54
Figure 33 Running phase (proteins separation).....	55
Figure 34 Result of the 1° test (on the left) and result of the 2° test (on the right).....	57
Figure 35 Result of the 3° test.....	58
Figure 36 Result of the 4° test (on the left) and result of the 5° test (on the right).....	59
Figure 37 Result of the 6° test.....	59

Figure 38 Result of the 7° test.....	60
Figure 39 Results of the 8° test	60
Figure 40 Result of the 9° test: coating shown over the bar without oxide layer (on the left) and coating shown over the bar with the oxide layer (on the right).....	61
Figure 41 Result of the 10° test (on the left-up), result of the 11° test (on the right-up) and result of the 12° test (down).....	62
Figure 42 Result of the 13° test (on the left-up), result of the 14° test (on the right-up) and result of the 15° test (down).....	63
Figure 43 Result of the 16° test (on the left) and result of the 17° test (on the right).....	64
Figure 44 hydroxyapatite-based coating on the bar from the 4° test	65
Figure 45 hydroxyapatite-based coating on the bar from the 5° test	65
Figure 46 hydroxyapatite-based double coating on the bar from the 8°	65
Figure 47 hydroxyapatite-based coating on the bar with the oxide layer from the 9° test.....	66
Figure 48 Black lines at high molecular weights show dimers and trimers.....	67
Figure 49 Molecular weight markers (on the left) and result of SDS PAGE (on the right)	67
Figure 50 A homogeneous and strong recoating on the bar, analyzed through a microscope, was observed after it underwent the procedure described in Experiment 5	69

List of Tables

Table 1 Main features of each test	47
Table 2 Main Characteristics of Spectrum Two.....	49

ABSTRACT

The use of titanium implants has been steadily increasing over the years. Titanium alloys, due to their distinctive properties, have gained widespread popularity in the field of implantology. Referring to titanium implants used in orthopedics, a crucial factor in ensuring long-term fixation and avoiding recurring issues such as mobilization and infections is the proper osseointegration between the implant and the host bone. This phenomenon is a recurring theme and subject to various studies, which focus on preparing the implant before its placement in the bone, ensuring a proper bond for the implant's longevity and preventing rejection by the human body. One method of preparing the implant before placement is to coat its surface with bioactive ceramics or hydroxyapatite, using various physical or chemical coating techniques, such as plasma spray or chemical vapor deposition, to name a few. These techniques create a rough layer composed of pores around the device's surface, allowing the bone tissue to grow into the holes, facilitating the fixation and stability of the prosthesis. However, there are still limitations to these techniques, leading to the need for further studies to find the optimal conditions for coating titanium implants that promote the best possible osseointegration.

The purpose of this study is to develop a procedure to provide a strong and as uniform as possible coating for titanium implants with heterologous equine bone tissue. Tests were conducted on grade 4 titanium bars and screws using two variations of equine bone powder. The procedure employed proved effective in two instances: by diluting the powder and combining it with an oxidative alkaline solution. Through IR analysis, it was possible to verify the chemical properties of the substance deposited on the implants. The obtained spectra indicate that the properties of the powder remain unaltered after treatment, affirming that the coating process does not adversely affect the bone powder. Subsequent SDS PAGE analysis further confirms that the collagen content of bone powder bound to the Titanium surface is unaltered, both in its primary and quaternary structure.

INTRODUCTION

1. TITANIUM AND TITANIUM-ALLOYS

In recent years, the prosthetic material that has entered the market in a big way is titanium, a material with excellent characteristics, including biocompatibility, corrosion resistance and lightness, which has made it useful in various applications, and in the medical field, for the production of prostheses and medical devices in orthopaedics and neurosurgery. Titanium ranks as the ninth most naturally occurring element in the Earth's crust and is commonly found in the form of oxide, within minerals such as rutile and ilmenite. Through a chemical process known as carbochlorination, titanium undergoes a reaction with chlorine and coke to produce titanium tetrachloride, followed by the addition of magnesium (Kroll process). The interaction between magnesium and titanium tetrachloride results in the formation of relevant chlorides and the production of spongy metallic titanium. Subsequently, the metallic titanium undergoes purification through successive melting processes and is then utilized either in its pure form or in combination with other elements to create titanium alloys. Notably, its mechanical properties enable the manufacturing of hip prostheses and dental implants [1]. As titanium may exist in more than one crystallographic form, it is classified as an allotropic element. At room temperature, titanium exists in the α -phase, also known as a hexagonal close-packed crystal structure (hcp). When this material in the solid state is heated to temperatures higher than 883°C or when it solidifies from a liquid, a transition from the hcp to the body-centered cubic (bcc) structure, or β -phase, becomes possible [2]. Various prior studies have demonstrated that alloying elements can significantly influence the phase transformation temperature of pure Ti. For this reason, alloying elements are typically categorized into α -stabilizers (such as Al, C, O) and β -stabilizers (such as Mo, Ta, Nb) [3]. Presently, while only 20 to 30 alloys have attained commercial status, more than 100 titanium alloys are known. Among the commercially used alloys, Ti-6Al-4V is the most widely utilized, covering over 50% of usage. Based on crystal structure, four classes of titanium alloys can be distinguished: α -alloys, near- α -alloys, ($\alpha+\beta$)-alloys, and β -alloys (*Figure 1*).

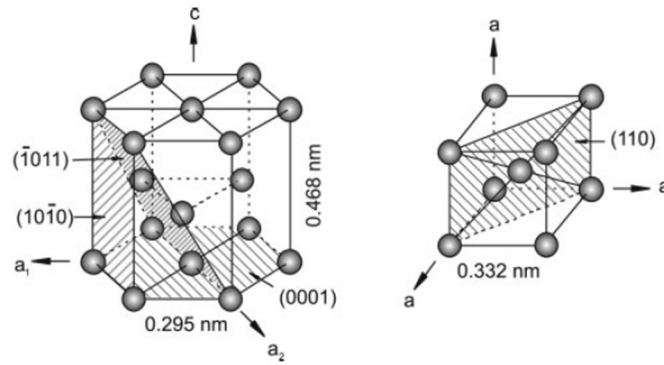


FIGURE 1 CRYSTAL STRUCTURE OF HCP A AND BCC B PHASE [4]

The α -alloys are defined by the exclusive presence of the α -phase and encompass four grades of commercially pure titanium and titanium alloys. These four grades of titanium exhibit variations in the content of Fe (ranging from 0.20 to 0.50 wt%) and O (ranging from 0.18 to 0.40). Near- α alloys, on the other hand, are essentially α -alloys that incorporate a small proportion of β -stabilizers (1-2 wt%), effectively stabilizing 5-10% of the beta-phase in the structure at room temperature [3] [4]. Both these classes share similar characteristics, including commendable weldability, high resistance to creep, and outstanding corrosion resistance. However, it is noteworthy that their strength at room temperature is relatively modest. The ($\alpha+\beta$)-alloys, featuring a higher concentration of β -stabilizers compared to near- α alloys, indeed manifest a more substantial fraction of the beta-phase (5-30 vol%). Diverging from α -alloys, this category of titanium alloys demonstrates favorable fabricability, elevated strength at room temperature, and the potential for optimizing mechanical properties through heat treatment. They still exhibit remarkable corrosion resistance and facilitate rapid osseointegration within the human body. Ti-6Al-4V belongs to this category, and these attributes contribute to its status as the most widely utilized biomedical alloy. β -alloys, with even greater amounts of β -stabilizers and lower levels of α -stabilizers, distinguish themselves by a reduced elastic modulus compared to other classes. They exhibit comparable strength, superior biocompatibility, and enhanced corrosion resistance within the human body. Consequently, numerous new beta-alloys with optimized properties for biomedical applications have emerged in the last two decades [3]. Consequently, by manipulating the type and quantity of alloying elements, it is feasible to create specific types of titanium alloys with distinct properties [4]. Due to their exceptional combination of properties, titanium and its alloys stand out as the preferred choice for manufacturing biomedical implants [3].

Titanium is essentially used in the biomedical field for its excellent characteristics such as [5]:

- High moment of inertia: no restrained sizes;
- High elastic module: more similar to the one of the bones, excellent property to minimise stress shielding problems;
- Low density: it is much lighter than other metals, thus providing less discomfort for the patient;
- High fatigue strength: it can withstand cyclic tensile and/or compressive loads without fracturing;
- High melting point;
- Low thermal conductivity;
- Low coefficient of thermal expansion: more compatible with ceramics and glass;
- Biocompatibility: no reaction from the body (rejection). Implants placed in the patient's bone will become one body with the bone, i.e. osseointegration takes place;
- Good corrosion resistance: titanium's ability to develop a passivating oxide layer on the surface. When the metal is exposed to oxidising environments, an oxide film characterised by good toughness, good adhesion and high stability forms spontaneously. The oxide is stable over a wide pH and temperature range, is only destroyed under strong reducing conditions and also has extraordinary resistance to chlorides, sulphites, sulphates and aqueous chlorates. Provided sufficient oxygen is present, the film can self-heal almost immediately. If mechanically damaged, contact with air leads to the rapid formation of a Ti oxide layer;
- Radio-opacity: clearly visible on an X-ray plate.

1.2. TITANIUM PROSTHESIS

As previously mentioned, Titanium is an excellent material that is used in the biomedical field and in particular for the manufacture of prostheses. It is possible to differentiate different types of titanium prostheses, such as:

- Joint prostheses:
 - Hip replacements: Titanium hip replacements are commonly used to replace the hip joint in patients with osteoarthritis or other conditions that cause pain and limit hip mobility.

- Knee replacements: Titanium knee replacements are used to replace the knee joint in patients with severe joint damage or deformity.
- Spinal Implants: Titanium is often used to make spinal fixation devices, such as screws, plates and rods, used in spinal surgeries to stabilize the spine after injuries or to treat conditions such as scoliosis.
- Cranial prostheses: In neurosurgery, titanium is used to create cranial prostheses. These prosthetics are used to repair and reconstruct parts of the skull that have been removed due to injury or surgery.
- Dental prostheses: Titanium is also used in dentistry for the creation of dental implants, which are used to replace missing tooth roots and anchor dentures.
- Prostheses for maxillofacial surgery: Titanium is used to produce craniofacial prostheses for patients who have suffered facial trauma or congenital malformations.
- Inner ear prostheses: In the field of otolaryngology, titanium can be used to make inner ear prostheses, for example for patients with cochlear implants.

To promote proper osseointegration, it is important to take various factors into account, such as:

- Biocompatibility;
- Characteristics of the implant surface and implant geometry: it is possible to have cemented implants, made of Cobalt, with smooth surfaces to better guarantee adhesion to the cement and favour compressive stress. If we talk about cementless implants, they are made of Titanium and the surfaces must be rough/porous to favour the formation of chemical bonds with the bone. In fact, curved protruding surfaces or surfaces with pores, which are comparable in size and radius to those of biological components, can induce different biological interactions than flat surfaces [6];
- Loading conditions: mechanical stresses are essential for correct integration of the implant, it is necessary to evaluate what is the appropriate loading intensity that favours remodelling of the bone in the presence of the prosthesis [7];
- Quality of the patient's bone: problems of osteoporosis and lack of certain minerals that make the bone more fragile could be detrimental to proper integration;
- Surgical technique chosen for implant placement.

1.2.1. ORTHOPEDIC IMPLANTS AND TITANIUM

ORTHOPEDIC IMPLANTS

Orthopedic implants are designed to restore both the structural integrity and functionality of compromised joints and bones. Achieving this objective necessitates the production of secure implants with a prolonged lifespan, minimizing the risk of rejection. As the body undergoes aging, bones may experience a decline in strength and elasticity, rendering them more susceptible to fractures. This vulnerability stems from the diminished mineral content in the matrix and a decrease in the flexibility of collagen [8]. When a bone fractures, the only recourse is to mend it by utilizing artificial support structures [9]. Additionally, accidents and joint-related ailments like osteoarthritis compel individuals to undergo surgical procedures that involve the use of implants, such as total hip and knee replacements [10]. Orthopedic implants can be defined as medical devices used to either aid or substitute damaged bones and joints by providing bone fixation or by replacing damaged articulating surfaces of a joint or a limb. They exist cementless or also called press-fit implants, that are implants made by titanium, coated with bio glasses to have a porous surface, or with a rough surface provided by the presence of divots, using for example grit blasting techniques or plasma spray techniques for the coating, that are pressed to fit so that bone can grow into the implant in force, establishing chemical reactions, or, in another case, they exist cemented type of implants, that are made by cobalt-based alloys and they show a smooth surface that is cemented into the bone channel.

Among the types of orthopedic implants, we can distinguish, based on their period of use, permanent implants, such as knee and hip prostheses. Depending on the type of issue, they can be total or partial replacements. In the case of hip prostheses, they are divided into arthroprostheses and endoprostheses, respectively, and for the knee, compartmental and unicompartmental prostheses, respectively. In particular, considering hip and knee prostheses, titanium is commonly used for the fabrication of non-cemented femoral stems (*Figure 2*). This choice facilitates the possibility of coating the stem and forming chemical bonds with the surrounding bone (osseointegration). The use of titanium in this application also promotes the transfer of mechanical stresses, particularly compressive stresses, as opposed to shear stresses, which enhances adhesion. Regarding knee prostheses, titanium is used in the fabrication of the tibial component. There exist also temporary implants, specifically used for the reduction and treatment of bone fractures, which include compression, support and neutralization plates, cortical, cancellous and cannulated screws, Harborview and Knowles pins, wires, and intramedullary rods, Kuntscher and Rush nails (*Figure 3*).

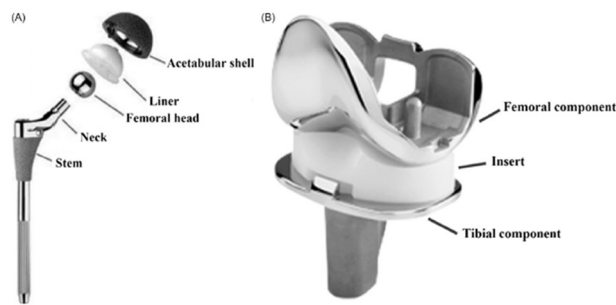


FIGURE 2 (A) TOTAL HIP AND (B) KNEE REPLACEMENT [10]

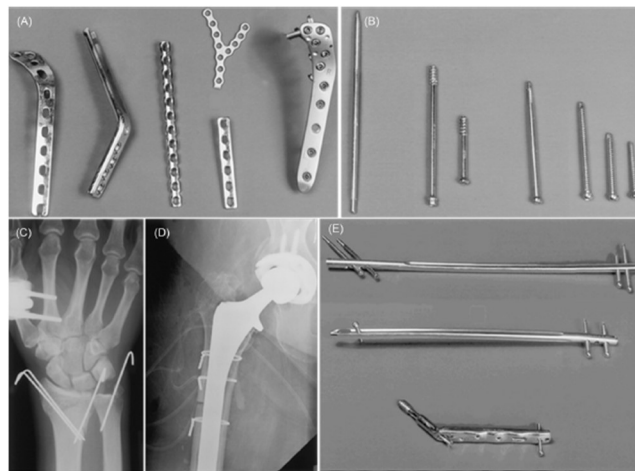


FIGURE 3 (A) PLATES, (B) SCREWS, (C) RADIOGRAPHIC SCAN OF IMPLANTED PINS, (D) RADIOGRAPHIC SCAN OF WIRE, (E) INTRAMEDULLARY RODS [10]

1.2.2. NEUROSURGERY IMPLANTS AND TITANIUM NEUROSURGERY IMPLANTS

Neurosurgery, a specialized field of medicine, focuses on surgical interventions within both the central nervous system and the peripheral nervous system. This involves procedures on the brain, spinal cord, spine, and nerves. The discipline is dedicated to the surgical diagnosis and treatment of various neurosurgical conditions, such as neoplasms, tumors, spinal disorders, scoliosis, hydrocephalus, epilepsy, dementia, and drug-resistant Parkinson's. In the neurosurgery field, titanium finds extensive use in the creation of diverse medical devices, including prostheses, plates, cranial screws, and other surgical instruments. Titanium is highly valued for its corrosion resistance, biocompatibility, and adaptability to be customized according to specific patient requirements [11]. In particular, its most popular applications are:

- Cranial protuberances: The skull is one of the most delicate bones in the skeleton and fulfils a very important function: protecting the brain. If, as a result of a serious accident, the skull breaks, it becomes necessary to undergo surgery to insert a prosthesis. Cranioplasty operations are therefore necessary whenever the patient's skull vault bone no longer provides a protective function for the underlying soft tissue. Causes can be traumatic events, degenerative diseases, bone resorption or infection following repositioning of autologous bone. Titanium is often used to create cranial prostheses, which are custom-designed to perfectly fit the shape of the patient's skull [12] (*Figure 4*);
- Vertebral fixation devices: Spinal surgery is now considered a true branch of orthopaedic surgery and neurosurgery. The aim of this branch is to restore the functions of the spinal column following trauma or degenerative or tumour diseases. Titanium is used to make screws, plates and rods used in spine surgery. These spinal fixation devices are used to stabilise the spine in patients with herniated discs, spinal deformities or spinal injuries [13] (*Figure 5*);
- Deep brain stimulation (DBS) electrodes: Neurosurgery uses titanium to produce electrodes that are implanted in the brain for deep brain stimulation. This procedure is used to treat patients suffering from neurological disorders such as Parkinson's disease, essential tremor and epilepsy;
- Intracranial implantable: Titanium is used to make intracranial implantable devices, such as catheters, cerebrospinal fluid reservoirs, drainage devices and valves used to treat hydrocephalus or other neurological conditions;
- Ear prostheses: Due to congenital malformations or injuries, titanium ear prostheses are used for reconstruction of the outer ear. Titanium is valued in prosthetics, and especially in neurosurgery, for its magnetic properties. This property is called paramagnetism, which refers to its ability to repel magnetic fields and generate a magnetic field opposite to the one applied. In practice, this property is a valuable feature in various engineering applications, including magnetic resonance imaging and magnetic simulation. For this reason, titanium implants are less likely to suffer complications from X-rays or CT scans. They also avoid being magnetised when exposed to electromagnetic fields, such as those produced by modern electronics. Although titanium has a limited magnetic field, its strong tensile strength makes it an important component for many industries. However, the implantation of a titanium alloy can have a slight impact on the MRI,

possibly affecting image quality, which must be thoroughly assessed by physicians according to the specific situation [14].

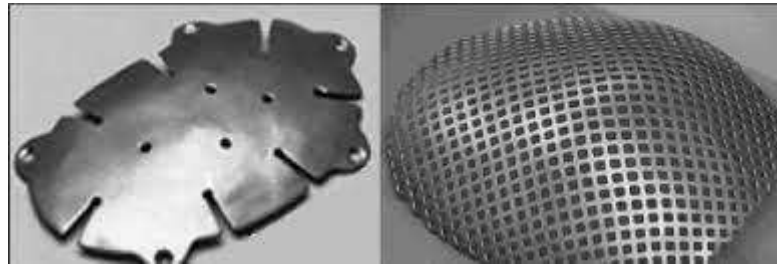


FIGURE 4 TITANIUM CRANIOPLASTY KIT: (A) TITANIUM PLATE, (B) TITANIUM MESH [48]



FIGURE 5 SPINAL FIXATION DEVICES[49]

2. CURRENT TITANIUM INTEGRATION TECHNOLOGIES

Osseointegration serves as the foundational process for implantology, precisely delineating the connection between a bone and an artificial implant without the presence of apparent connective tissue. Coined in the late 1960s by Dr. Branemark, a professor at the Institute of Applied Biotechnology in Gothenburg, the term "osseointegration" has since become widely recognized, and Dr. Branemark is acknowledged as the pioneer of modern implantology. Through his research, it was observed that titanium, when in contact with bone, develops an oxide on its surface, facilitating the 'adhesion' between the implant and the bone itself. Subsequently, implantology underwent significant advancements, leading to the development of new, more effective surfaces aimed at enhancing the osseointegration process [15]. The

osseointegration factor, that creates a stable connection between the bone and the prosthetic device, is the crucial part when it comes to prostheses; on the other hand, however, it is also one of the most discussed and difficult to achieve optimally, as it depends on several factors. The bone integration is essential for the prosthetic implant to be stable and functional in the long term. The patient's bone health plays an important role in osseointegration. It is important to have a healthy lifestyle, eat a balanced diet, with calcium and vitamin D supplementation if necessary [16], as well as control of conditions such as diabetes and osteoporosis, a systemic skeletal disease that increases bone fragility and susceptibility to fractures, as it involves deterioration of the microarchitecture of bone tissue and a reduction in bone mass. Practitioners often promote bone health as an integral part of the implantology process. Continuous monitoring of bone health is extremely important, especially for patients with osteoporosis, including through post-operative follow-up, to ensure that osseointegration is progressing correctly, and if there are any problems, to act promptly. Several techniques have been developed to compensate for the lack of osseointegration, to promote it or to improve it. For this, improvements are continuously implemented. In this area, the investment in research and development by manufacturers is continuous, in order to develop an appropriate design and choice of materials used to manufacture implants, to reduce the risk of implant rejection and to improve bone integration capacity. Improved surgical techniques for implant placement can also be decisive. They aim to be effective and minimally invasive, so that the implant is inserted correctly into the site and ensure its stability to avoid aseptic loosening, for example. Also crucial is the training and education of professionals in the field, who must be trained to apply best practices in the management of prosthetic implants, while remaining informed of the latest developments in implantology, osseointegration and materials science.

As for regard the modern days, the integration of titanium use in medical applications is constantly evolving. The market for osseointegration technologies continues to grow and evolve, with an increasing emphasis on customisation, materials science and the adoption of evidence-based approaches to improve implant success and patient well-being. The initial approach is based on a specific evaluation and diagnosis by the doctor to create a custom-made prosthesis in order to have a customised implant. This in particular is done with the use of innovative techniques, for example through CAD/CAM (Computer-Aided Design/Computer-Aided Manufacturing) technology, which allows the design and production of implants customised to perfectly fit the patient's anatomy, improving osseointegration and reducing the risk of complications. This type of approach allows prosthetic finalisation in a predictable manner, with reduced treatment time, providing significant advantages to clinician and patient

from this point of view [17]. First of all, the anatomical data are acquired through a Reverse Engineering (RE) process using diverse scanning systems to acquire the anatomical shape in CAD format, like mechanical tracker, optical fringes-based methods, laser based scanning, radiographic acquisition (CT, MRI). After the scanning, the image is saved in a DICOM format, it is imported in a software available on the market such as MIMICS or DentalVox and then the model is virtually generated. Then, the latter is manufactured using Solid Freeform Fabrication (SFF) techniques that, depending on the final result that is to be achieved, they can be used Electron Beam Melting (EBM) or Direct Metal Laser Sintering (DMLS) technologies. At the end of the procedure a customized titanium implant has been obtained where surface finishing modifications can be made to optimize biocompatibility and osseointegration.

Other techniques to which titanium can be subjected and which promote its integration into prosthetic use involve surface coating techniques with bioactive materials such as hydroxyapatite or zirconium dioxide to increase the adhesion of bone cells to the implant and accelerate the healing process, or subjecting the metal to specific surface finishing treatments, including mechanical treatments, such as machining, surface polishing and sand-blasting, chemical treatments, using acids, thermal treatments, laser and vacuum treatments, to obtain a textured surface of the finished product.

3. OSSEOINTEGRATION FAILURE

Despite the innovative techniques and materials used in the production of prosthetics, the longevity of the implant can be reduced due to various factors. Taking total joint replacement as an example [18], the causes of its failure can occur in an early stage (less than 10% of cases), in the case of dislocation or infection, or approximately 5 years after surgery. In the case of dislocation, when the bone fails to grow onto the components or the cement loosens over time, the patient will experience pain, and the joint can become unstable or loose. Hip replacement dislocations occur in about 4% of first-time surgeries and about 15% of revision hip replacements (*Figure 6*). Factors that may increase the chances of hip or knee joint loosening include:

- excess body weight (obesity), which puts strain on the joint components;
- high-impact activities or exercises;
- wear and tear of components over time.

Most initial hip or knee replacement parts are designed to last 15 to 20 years. If a patient undergoes replacement surgery at a younger age, they may be more likely to need revision

surgery later as the components naturally wear out over time. In the case of prosthetic joint infections, bacteria organize into structures called biofilms. In this state, the bacteria are thousands of times more resistant to growth-dependent antimicrobials. Bacteria become organized within the biofilm with structural and functional heterogeneity along the surface of the prosthetic material and are resistant to attacks from the immune system, allowing them to grow and proliferate freely. Most infections will require revision surgery.

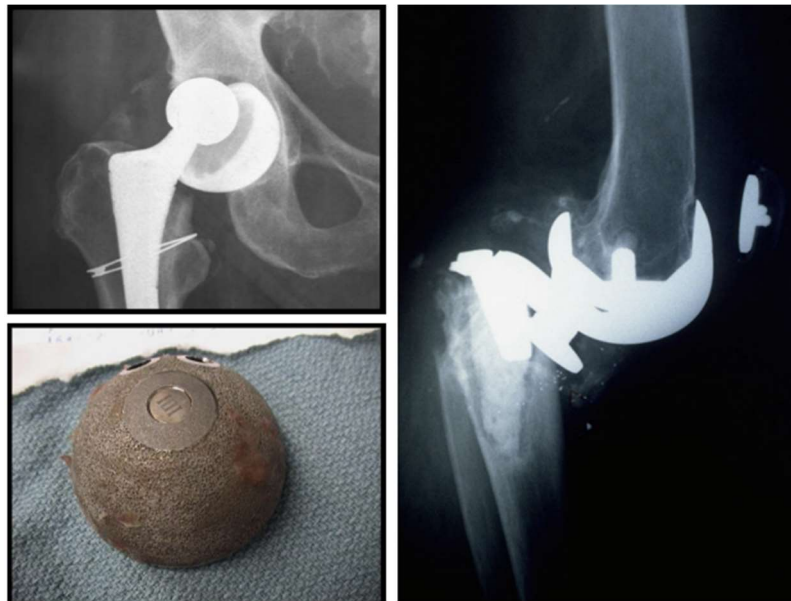


FIGURE 6 EXAMPLES OF IMPLANT FAILURE [50]

These infections are rare, occurring in 1% to 2% of patients. But given that joint replacement surgery has become one of the world's most common elective procedures, this means that thousands of people are affected each year. The most common symptoms associated with loosening or instability in the hip or knee joint include pain, clicking sound, sensation that the joint is moving in and out of its socket, partial hip dislocation (subluxation), full hip dislocation, swelling.

The long-term failure causes are related to the wear of the articular bearing surface, osteolysis, mechanical loosening, and peri-prosthetic fracture. Wear of an articular bearing surface is one of the main causes of failure after five years from the date of implant, and often wear is accepted as a natural consequence of use. Wear occurs in four different modes depending on the location (*Figure 7*).

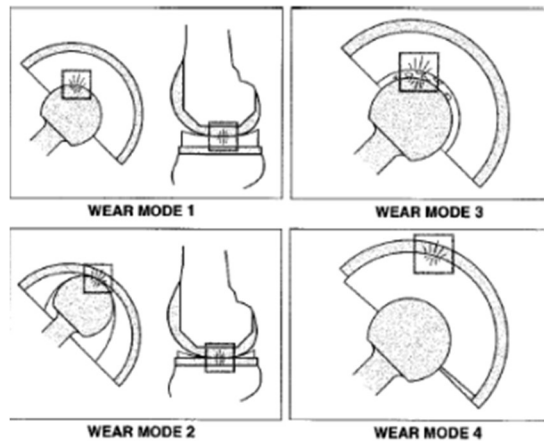


FIGURE 7 MODE 1 IS THE ONLY WEAR MODE ASSOCIATED WITH JOINT ARTICULATION, IT OCCURS AT THE INTENDED BEARING SURFACES (FEMORAL HEAD AND ACETABULAR CUP). MODES 2, 3 AND 4 OCCUR AT OTHER NONINTENTIONAL ARTICULATIONS AS A FUNCTION OF PROSTHESIS MATERIALS, DESIGN AND IMPLEMENTATION MODE. [51]

In general, the four major wear mechanisms are abrasion, adhesion, surface fatigue and chemical reactions.

Another problem is the osteolysis, that is the process of progressive destruction of periprosthetic bony tissue, and is a serious complication of total hip replacement in the medium to long term. Although often asymptomatic, osteolysis can lead to prosthesis loosening and periprosthetic fracture. Due to corrosion between materials, between bone and material, or due to other factors, there is a production of debris, which activates the immune system to remove the debris, but in doing so, it also engulfs the bone in the area of the prosthesis, and from this bone loss, implant loosening results, a condition whereby the prosthesis no longer has enough bone to hold onto. These complications cause significant morbidity and require complex revision surgery. Another problem related to the failure can be the periprosthetic fractures, for which the bone around the implant stem can break in many different ways [19] (*Figure 8*).

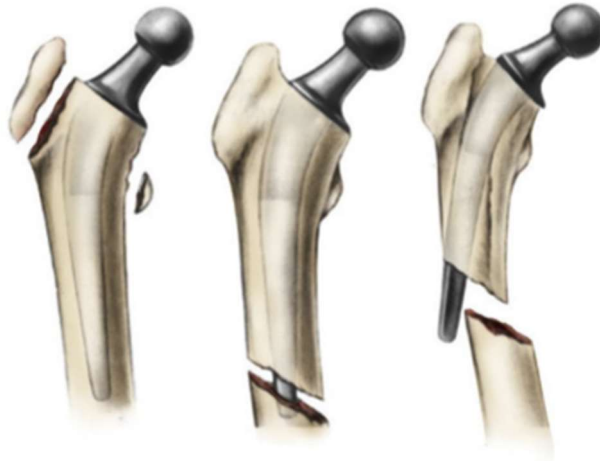


FIGURE 8 PERIPROSTHETIC FRACTURE [52]

At a generic level, there are many factors that compromise osseointegration. These include the bone problems that may afflict the patient, such as bone shortage, osteoporosis and bone atrophy; the healing time required for the implant to be completely anchored in the bone, which should be minimal; infections and complications due to incorrect surgical techniques; coupling of the right materials, which if incorrect, could lead to corrosion problems and its side effects, which would then also affect long-term stability. In any case, the scientific field of research is constantly developing to find the best techniques to overcome these problems.

4. IMPLANT COATING TECHNIQUES

Surface treatments are used to selectively modify the properties of biomaterials and therefore, to improve devices' multifunctionality, their tribological and mechanical properties. In this way, it is possible the enhancement of device performances that are often finalized in the achievement of better integration of the implant within the biological tissue [20]. The coating of the implant surface is an additive method, which means that other materials/agents of various thicknesses are superficially added to the surface of the core material [21].

There are different types of coating and in particular, referring to osseointegration, we can discern:

- Osteoconductive coatings, drive bone formation to grow or attach to the surface of the coating (passive coatings) [22];
- Osteo-inductive coatings, induce the bone formation of undifferentiated cells in the surrounding tissue to ultimately promote osseointegration of bone to the coating (active coatings) [22].

Moreover, various studies affirm that the surface roughness of titanium implants significantly influences the rate of osseointegration and biomechanical fixation [23][24]. There are three noteworthy levels of roughness: macro-, micro-, and nano-sized. The macrolevel is directly associated with implant geometry, and numerous studies have underscored the correlation between this type of roughness profile and the early fixation as well as the long-term mechanical stability of the implant/prostheses in comparison to a smooth implant surface. The micro-level of roughness has been observed to enhance the interlocking between mineralized bone and the implant surface. Roughness in this range results in increased bone-to-implant contact and greater resistance to torque removal compared to other surface topographies. Consequently, it is predominantly employed in cases of poor quality or volume of the host bone. The ideal microscale surface roughness should feature hemispherical pits with a depth of 1.5 μm and a diameter of 4 μm . Roughness profiles in the nanometer range play a crucial role in the selective adsorption of proteins, leading to the adhesion of osteoblastic cells and influencing the rate of osseointegration. However, achieving reproducibility of this specific surface roughness through chemical treatments poses challenges, and the optimal nanoscale surface roughness remains unknown [23][24]. Although numerous methods have been developed to modify the surface of implants and prostheses in order to enhance their properties and to create a rough surface leading to better osseointegration. The vast majority of techniques used involve covering the substrate with a thin layer of material, which, depending on the end purpose, may be bioceramics, bioglass or other materials that promote bioactivity. To do this, there are both chemical and physical methods.

4.1. PHYSICAL DEPOSITION METHODS

Physical methods, which compared to chemical methods offer purity of coverage, good strength and durability and are environmentally friendly, are however more expensive because they require the use of special machinery and specialised personnel, resulting in a coverage that is in any case not as uniform and strong as that formed with the chemical method, since no chemical bonds are formed between the substrate and the covering material.

4.1.1. PLASMA SPRAY

Plasma spray processes exploit the energy contained in a thermally ionized gas to melt partially and propel fine powder particles of metallic or non-metallic materials onto a surface so that they adhere and agglomerate to produce coatings [25] (*Figure 9*). Consequently, plasma coatings result from the agglomeration of splats formed by the impact, spread, and solidification

of individual particles. The process may be at atmospheric pressure or under vacuum and the heat source for melting and accelerating the powders can be direct current plasma (DC-P) or radio frequency inductively coupled plasma (rf-ICP) [26]. Since the splat shape is dependent on several factors such as powder material properties, impact conditions, impact velocity, temperature, etc., to obtain a good quality coating the spray parameters must be selected carefully [26]. Several are the kinds of the plasma source, but the more common are the metallic, gaseous, and laser-based plasma sources [27]. The plasma spray torch is the device that produces and sustains a high-temperature confined region so that powder molecules injected into that region can be heated and accelerated onto a workpiece. The concentration of the power of an electric arc in an extremely small volume allows the achievement of high temperature, while the appropriate design of the spraying nozzle provides acceleration [25]. Bioactive ceramics, such as hydroxyapatite, are widely used in the plasma spray process as interfacing osteoconductive layers in metallic surgical implants [27]. Plasma sprayed coatings are generally much denser, stronger and cleaner than the other thermal spray processes. Complex geometry specimens can be suitably treated; the wide spectrum of materials that can be used with this technique has stimulated applications in the area of high-temperature, corrosion resistant, and ablation resistant coatings as well as biocompatible films. Plasma spray coatings probably account for the widest range of thermal spray coatings and applications and makes this process the most versatile. The disadvantages of the plasma spray process are relative high cost and complexity of the process. Respect other chemical treatments, it presents poor coating-substrate adherence, that makes necessary pre-treatment able to guarantee a minimum adhesion of coating.

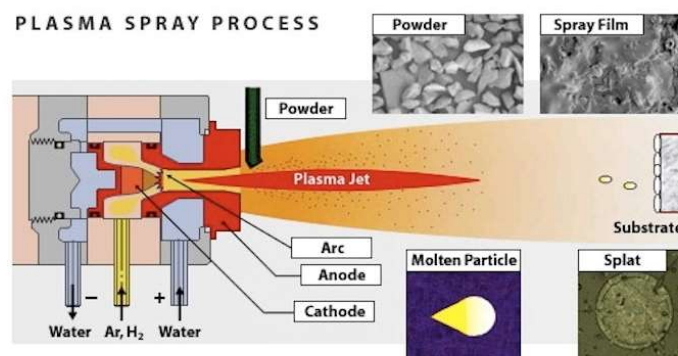


FIGURE 9 PLASMA SPRAY EQUIPMENT [53]

4.1.2. PULSED LASER DEPOSITION

Pulsed Laser Deposition is a process which involves focusing of a high intensity pulsed laser beam on the source material to be deposited on a substrate inside a chamber under high vacuum condition. The source material is subjected to ablation and this causes particles to detach from the material itself, and they are ejected as a plasma plume from the target. They then collide on the substrate, positioned in front of the target material, and stick, creating the overlay thin film (*Figure 10*). The PLD process is carried out in either presence of a background gas or under an extremely high vacuum. The interaction between the laser and the target and the film-growth processes, however, are very intricate physical phenomena. Sequences of energy conversion processes are necessary for films to grow using the PLD approach. Particle exfoliation, ablation, plasma generation, and evaporation are all effects of the PLD technique's process of energy conversion [28]. The pros of this technique is that it's flexible, because it can be used also with complicated materials, easy to implement, it can be used in every environment and by controlling the number of pulses, a fine control of film thickness down to atomic monolayer can be achieved. It's possible to achieve a high control of growth by varying laser parameters. The problems that can be encountered with this technique, however, are the uneven coverage, the high defect or particulate concentration, and in particular, one of the major problems is the splashing or the particulates deposition on the films (droplets), that which can become sites of stress concentrations leading to the formation of cracks on the surface. It's not well suited for large-scale film growth.

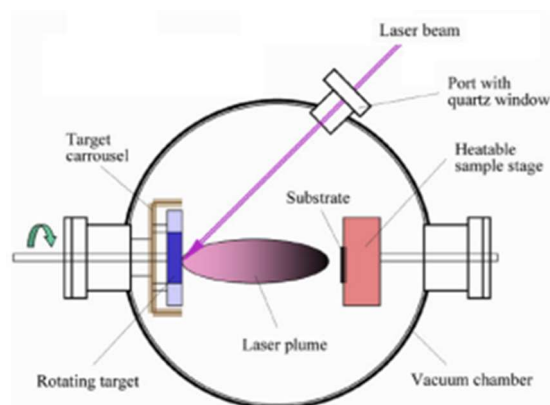


FIGURE 10 PLD EQUIPMENT [54]

4.2. CHEMICAL DEPOSITION METHODS

Chemical deposition methods allow a more precise control over the thickness and the composition of the film, due to the controlled chemical reaction involved, for this reason, it can be used for the coating of complex structures. The film that is formed it shows high purity and good adhesion. Due to the use of chemicals, the dangerous by-products formed need to be eliminated (i.e. HCl). Carrying out this type of technique in any case remains less expensive and less complicated than physical ones, because it is not necessary to have specific equipment.

4.2.1. CHEMICAL VAPOR DEPOSITION

Chemical vapor deposition (CVD) is a process whereby a solid material is deposited from a vapor by a chemical reaction occurring on or in the vicinity of a normally heated substrate surface. The resulting solid material is in the form of a thin film, powder, or single crystal (*Figure 11*). By varying experimental conditions, including substrate material, substrate temperature, and composition of the reaction gas mixture, total pressure gas flows, materials with a wide range of physical, tribological, and chemical properties can be grown [29]. The deposition occurs due to a chemical reaction between some reactant gases on the substrate, called precursors, that are pumped into a reaction chamber, the reactor. Under specific conditions of pressure and temperature, the precursors undergo to decomposition, breaking down into reactive species, such as ions. These ions, the products of the reaction, are deposited on the substrate, while the by-products are pumped out. The thin film continues to grow layer by layer, conforming to the substrate's shape.

They exist various types of CVD, depending on the working conditions used [30]:

- Thermal-CVD;
- Photo Assisted-CVD (PECVD);
- Plasma Enhanced-CVD (APCVD);
- Low Pressure-CVD (LPCVD);
- Metalorganic CVD (MOCVD).

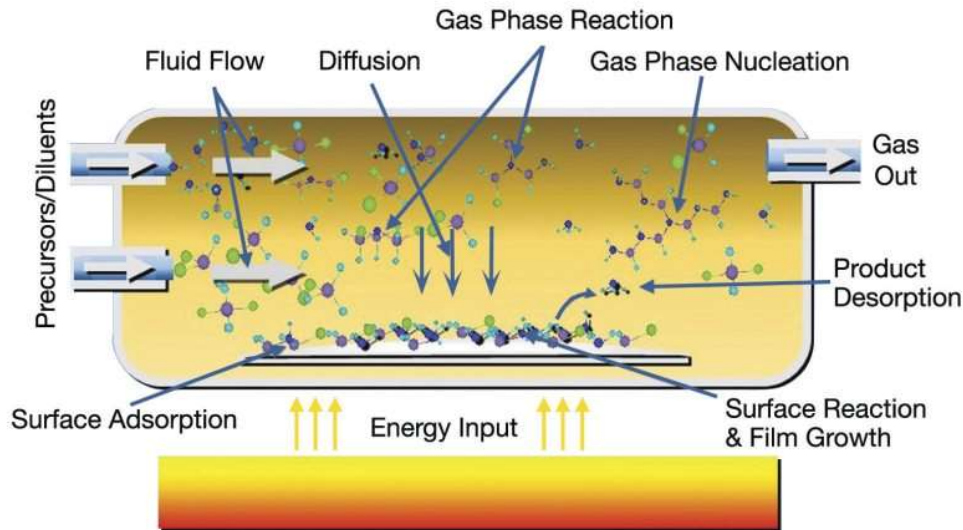


FIGURE 11 CVD EQUIPMENT [55]

4.2.2. SOL GEL PROCESS

Sol-gel process provides a new approach to the preparation of new materials. Homogenous multi-component systems can be easily obtained; in particular homogenous mixed oxides can be prepared by mixing the molecular precursors solutions.

The chemistry of the sol-gel process is based on hydrolysis and polycondensation reactions. Metal alcoxides $[M(OR)_3]$ and metal chlorides are versatile precursors used to obtain oxides, on account of their ability to form homogeneous solution in large variety of solvents and in the presence of other alcoxides or metallic derivatives and also for their reactivity toward nucleophilic reagents such as water [31]. The process involves conversion of monomers into a colloidal solution (SOL) that acts as the precursor for an integrated network (GEL) of either discrete particles or network polymers. The sol is defined as the colloidal (size ranging from 1 nm to 1 μ m) or molecular suspension of solid particles of ion in a solvent. The gel is a semi-rigid mass, three-dimensional network that forms when the solvent from the sol begins to evaporate and the particles or ions left behind begin to join together in a continuous network. First of all, the preparation of the sol is carried out, dispersing the precursors in a solvent. The precursors contain the elements that will form the desired material. Then, in the sol, the precursor molecules undergo to hydrolysis and polycondensation process, through which they link together through chemical bonds to form the gel, an inorganic three-dimensional network containing a liquid phase. After, a drying process is carried out to remove the liquid phase from the gel, thus forming a porous material, followed by a thermal treatment (firing), that may be

performed in order to favour further polycondensation and enhance mechanical properties. The result of a sol-gel process is often a solid material, such as ceramic, glass, or thin film, with controlled properties of composition, porosity and microstructure [32] (*Figure 12*). The sol-gel process offers several advantages, including the ability to realize materials with controlled nanostructure, with corrosion protection performances, good porosity and high purity and homogeneity with a low price. In addition, it can produce a thin bond-coating to provide excellent adhesion between the metallic substrate and the topcoat. In the gel state, it can easily shape materials into complex geometries.

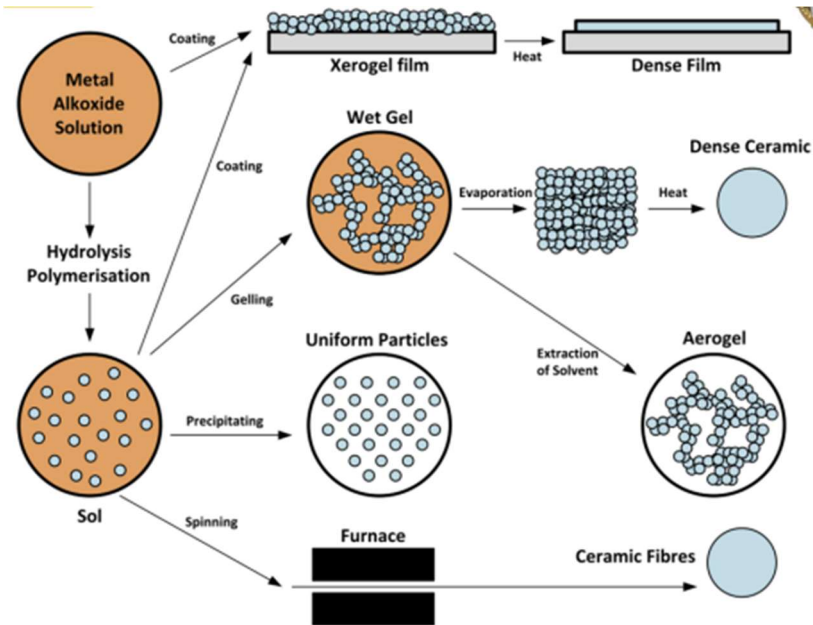


FIGURE 12 SOL-GEL PROCESS [56]

4.2.3. DIP COATING

Dip coating and spin coating methods are frequently employed to produce thin films from sol-gel precursors for research purposes, where it is generally used for applying films onto flat or cylindrical substrates [33] (*Figure 13*). The sol-gel technique creates films of increased, precisely controlled thickness that are mainly determined by the deposition speed and solution viscosity. In general, dip coating refers to the immersing of a substrate into a tank containing coating material, removing the piece from the tank, and allowing it to drain. The coated piece can then be dried by force-drying or baking [34]. The process is following three main stages:

- Dipping of the substrate into the coating solution: the coating material is dispersed in a solvent to create a coating solution, then the substrate is carefully immersed in the solution;
- Withdrawal: the substrate is slowly withdrawn. A thin film layer of the coating material, that depends on the withdrawal angle, adheres to the surface;
- Gelation of the layer by solvent evaporation to stabilize the coating.

Many factors contribute to determining the final state of the dip coating of a thin film. Different kind of dip coated film structures and thicknesses can be fabricated by controlling many factors: functionality of the initial substrate surface, submersion time, withdrawal speed, number of dipping cycles, solution composition, concentration and temperature, number of solutions in each dipping sequence, and environment humidity. The dip coating technique can give uniform, high quality films, bulky and complex shapes.

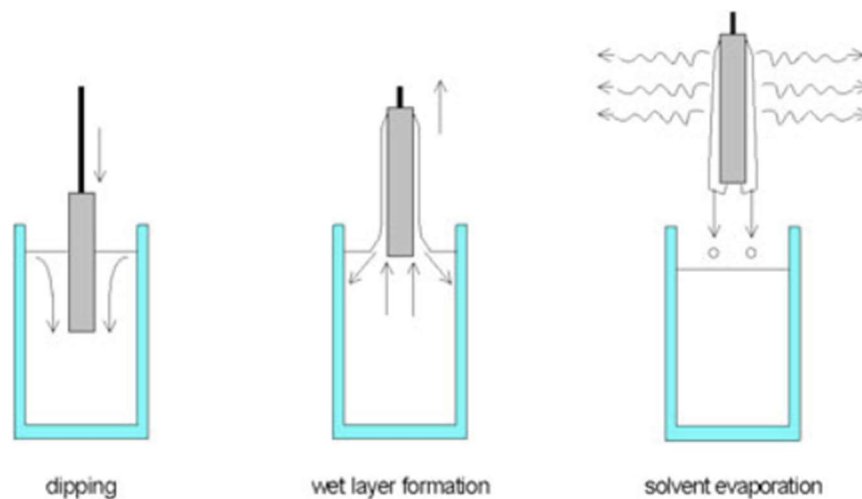


FIGURE 13 STAGES OF THE DIP COATING PROCESS [21]

4.2.4. SPIN COATING

Spin coating is a popular way of creating thin film coated materials along with the dip coating procedure (*Figure 14*). The working principle of this method is this :

- A drop of the liquid coating material is dispensed onto the centre of a surface placed over a machine, called spin coater, or simply spinner [35];

- The substrate is then rotated at speeds up to 10,000 rpm to spread the coating material outward by centrifugal force. Rotation is continued while the fluid spins off the edges of the substrate, until the desired thickness of the film is achieved;
- As the substrate continues to spin, the solvent present in the coating material gradually evaporates leaving a uniform and thin film;
- Once the solvent is completely evaporated, the coating material solidifies.

The viscosity and the concentration of the fluid are two important characteristics on them depend on the thickness of the film during the deposition. The latter is also dependent on the angular speed of the spinning, in fact higher is the speed, thinner will be the film. One advantage of the spin coating technique is that is possible to form a thin layer that is pure and uniform, in which, usually, the thicknesses do not vary more than 1%.

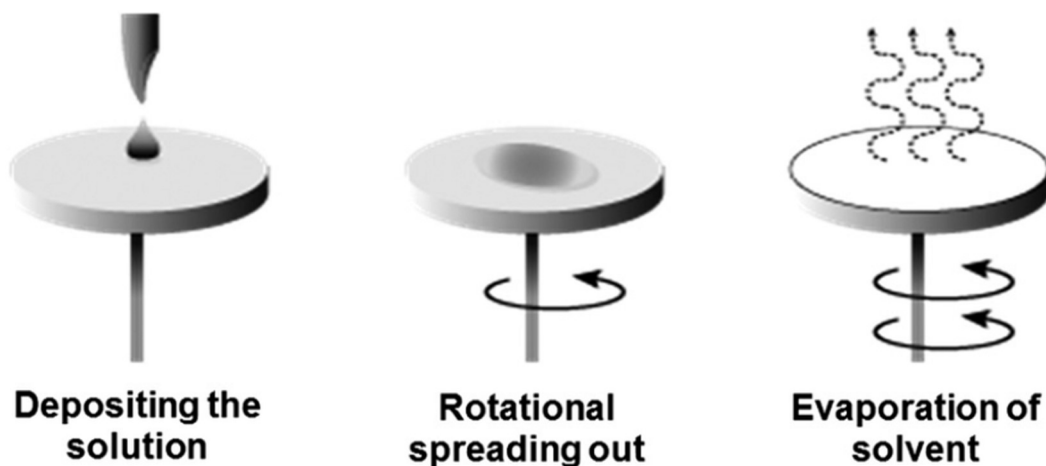


FIGURE 14 SPIN COATING PROCESS [57]

4.3. CHIMERA COATING

The coating process described is utilized for the enhancement of screws, implants, and prostheses crafted from titanium and its alloys. What sets this process apart is its reliance on decellularized bone tissue (whether autologous, homologous, or heterologous) containing native extracellular matrices. Despite the numerous advantages of titanium implants, such as high resistance to corrosion, low specific weight, sufficient durability, and excellent biocompatibility, a significant drawback is their inability to form a chemical bond with bone tissue. Over time, this limitation can lead to implant loosening or bone slippage, resulting in damage to the adjacent tissue. To address this issue, continuous efforts are made in the

development and adoption of surface coatings. However, commonly used techniques like plasma spray have limitations, providing poor binding and proving to be complex and expensive. Moreover, the incorporation of organic materials, such as bone tissue, to improve osseointegration through the presence of an extracellular matrix is not feasible using existing methods. The Chimera coating method stands out due to its activation of decellularized and de-antigenated mammalian bone tissue, preserving the native form of the extracellular matrix without denaturation. The process involves preparing bone tissue to obtain a powder, which is then suspended in an aqueous solution containing 10-35% volume of hydrogen peroxide. This suspension is maintained at a temperature between 10 to 30°C for a contact time ranging from 10 minutes to 4 hours, in a ratio of 1:1 by weight. Subsequently, the titanium metal substrate is introduced into this solution for a maximum time of 5 minutes. What makes this process unique is the absence of prior documentation indicating the simultaneous presence of bone powder and the metal implant in a hydrogen peroxide aqueous solution. This step is posited as crucial for the formation of more durable, covalent bonds, enabling the titanium implant to securely integrate with the suitably prepared bone tissue. This innovative coating procedure is detailed in the patent published by Tiss'you SRL Regenerative Company on the "Patentscope" online platform on 11.02.2021. The publication, identified as WO/2021/024197, is titled "Process for coating implants, plates, screws, or prostheses made of titanium and its alloys with decellularized bone tissue (autologous, homologous, or heterologous) containing native extracellular matrices."

5. COATING MATERIALS

Depending on the type of technique used, factors related to biocompatibility, desired application, functional requirements of the device, chemical resistance and mechanical strength, different target cover materials can be used [36][37][38][39].

Beginning with physical deposition methods, which are thin-film deposition techniques involving the transfer of material from the vapour phase to the solid phase, the deposition materials on the substrate can be:

- Aluminium (Al): non-magnetic, has reflectivity and high electrical, thermal and sound conductivity, light weight and low elastic modulus, similar to bone;
- Gold (Au): high electrical conductivity, chemically inert, aesthetically attractive, heavy, ductile, malleable, yellow in colour;
- Titanium (Ti): light, corrosion-resistant, tough, stiff, low density, biocompatible;

- Platinum (Pt): white metal, lustrous, ductile, malleable, chemically inert, high electrical conductivity;
- Silver (Ag): high electrical conductivity, lustrous white metal, soft, ductile and malleable;
- Copper (Cu): excellent electrical and thermal conductivity, corrosion resistance, ductile, malleable;
- Chromium (Cr): very hard grey metal, brittle, durable, corrosion resistant, can be easily ground and polished;
- Tungsten (W): high melting point, durable;
- Nickel (Ni): durable, easily machined, corrosion resistant;
- Zinc (Zn): good corrosion resistance, brittle and crystalline at ordinary temperatures, but becomes ductile and malleable when heated between 110°C and 150°C.

In chemical deposition methods, thin-film deposition techniques involving the chemical reaction of precursor gases on the surface of a substrate to form a solid material, the overlay materials used in these processes, which affect the thickness of the deposited film, can be:

- Polycrystalline Silicon (poly-Si): good electrical properties;
- Diamond (C): extreme hardness, high thermal conductivity;
- Aluminium (Al): light, good electrical conductivity;
- Silicon Oxide (SiO₂): excellent electrical insulator;
- Silicon Nitride (Si₃N₄): high-performance technical ceramic, with high strength, toughness and hardness, extremely resistant to thermal shock and impact, high thermal resistance, good wear resistance;
- Graphene: high mechanical strength;
- Tantalum (Ta): hard and ductile, shiny, blue-grey transition metal, very resistant to corrosion, especially to acid attack, good conductor of heat and electricity, high density;
- Silicon Carbide (SiC): low density, excellent hardness, very good corrosion resistance in both acid and alkaline environments, high thermal resistance, chemical stability;
- Ruthenium (Ru): corrosion resistance, high electrical conductivity;
- Amorphous carbon thin films (a-C): flexible, transparent, wear-resistant.

The selected covering materials can vary depending on specific applications and required standards. In general, from a broader perspective, those favoured in the biomedical field are:

- Silicone: excellent mechanical properties, high resistance to irradiation, biocompatible, resistant to low temperatures;
- Thermoplastic Polymers (PVC (polyvinyl chloride), PE (polyethylene), PP (polypropylene)): the characteristic that distinguishes them is their malleability when heated and return to the solid state when they cool, flexibility, chemical resistance and biocompatibility, wear resistance, excellent electrical, thermal and acoustic insulation, transportability and ease of use thanks to the light weight of the material;
- Teflon (Polytetrafluoroethylene, PTFE): anti-adhesive and non-stick, low friction coefficient even in the presence of high loads, high chemical resistance, biocompatible;
- High density polyethylene (HDPE) and low density polyethylene (LDPE): flexible, resistant, biocompatible;
- Polyurethanes (PU): does not flake, does not age or discolour, resists any environmental condition and consequently can also be applied in environments rich in saltiness and humidity, inert, does not rot and is not penetrated by water, flexible, biocompatible, resistant to abrasion;
- Titanium: Lightweight, resistant, biocompatible;
- Stainless steel: corrosion resistant, robust, high temperature oxidation (flaking) resistance and good mechanical strength at high temperatures;
- Glass or glass-ceramic: high resistance to thermal stress and abrasion, inert, corrosion-resistant, transparent;
- Polymethyl methacrylate (PMMA): transparency and surface shine, rigidity and dimensional stability, hardness, excellent resistance to ultraviolet radiation and ageing, biocompatible.
- Nylon: flexible, high abrasion resistance, high thermal stability, very good mechanical strength and hardness, high mechanical damping characteristics, biocompatible.

6. ANALYTIC TECHNIQUES

6.1. SDS PAGE

SDS-PAGE (Sodium Dodecyl Sulphate - PolyAcrylamide Gel Electrophoresis) is an analytical technique that allows the analysis of protein extracts. It is the most widely used technique in the qualitative analysis of protein mixtures. To perform this technique, sodium dodecyl sulphate

(SDS) is used, which is an anionic detergent that denatures the proteins by giving them the same (negative) charge density and binds to them, and for every 2 Aa binds an SDS molecule, destroying almost all non-covalent interactions. In this way, the protein chains are unwound and become almost linear, presenting an overall negative charge proportional to their mass. Furthermore, the addition of reducing agents such as dithiothreitol (DTT) or 2-mercaptoethanol causes the reduction of any disulphide bonds present between the cysteine residues. A polyacrylamide gel support is used to perform the protein separation. Polyacrylamide gels are the media that are used due to their chemical inertness and porosity properties, which can be controlled by varying the percentage of acrylamide and bisacrylamide, which form cross-links in the polymerisation process. Afterwards, the SDS-protein complexes are subjected to electrophoresis in a polyacrylamide gel, which contains SDS, and during the process, their migration to the anode and separation according to their molecular weight, caused by the molecular sieving of the polyacrylamide gel due to the pore size of the gel, is visible. This leads to smaller proteins migrating faster through the gel, while those of larger proteins migrate more slowly. In SDS-PAGE, a discontinuous gel is used, consisting of stacking gel, which is the upper part of the gel and is the part in which the wells in which the samples to be analysed are deposited are formed, which has the function of compressing and concentrating the protein components, and running gel, which is the lower part, and is the matrix capable of separating the individual macromolecules, in which the actual separation takes place. The samples to be analysed must first be solubilised in a buffer containing SDS, reducing agents (e.g. β -mercaptoethanol), a thickener (sucrose or glycerol) and a coloured tracer (bromophenol blue to follow the electrophoretic course [40][41] (*Figure 15*).

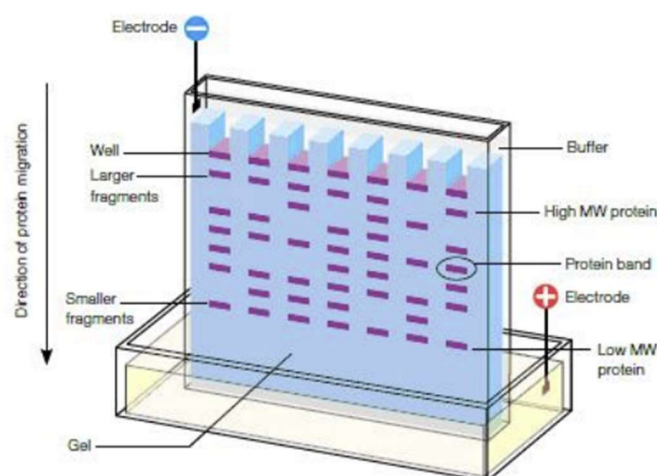


FIGURE 15 SDS-PAGE EQUIPMENT [41]

6.2. IR Spectroscopy

Spectroscopy is the scientific study that aims to identify the specific energies and quantities of incident light absorbed and subsequently re-emitted by particular substances. Infrared (IR) spectroscopy is particularly valuable for indicating the presence or absence of specific functional groups. If two pure samples exhibit the same IR spectrum, it can be inferred that they are the same compound [42]. Spectrometers, the optical instruments, unveil the absorbed and emitted light energies, producing spectra consisting of specific wavelengths or frequencies. These spectra provide crucial insights into the atomic and molecular structure of focused substances, essentially serving as unique "fingerprints" for different compounds [43]. One of the most prevalent spectroscopic techniques is Infrared (IR) spectroscopy, an analytical method available to today's chemists [44][45]. It relies on the molecular vibrations of a molecule, with the spectrum obtained by passing infrared radiation through a sample and determining the absorbed portion of the incident radiation at specific energies. Peaks in the absorption spectrum correspond to the energy associated with the vibration frequency of a segment of a sample molecule [46]. This analysis aims to identify the chemical functional groups within the sample [44]. A crucial requirement for a molecule to exhibit absorption in IR radiation is that it must possess an electric dipole moment that changes during vibration [45][46]. Vibrations involve changes in bond length (stretching) or bond angle (bending) in molecular dipoles. Molecules can absorb incoming infrared radiation only if its frequency matches one of the fundamental vibration modes of the molecule, enhancing the vibrational motion of a specific part while leaving the rest unaffected. Additionally, the greater the change in the dipole moment, the more intense is the absorption band [45]. The total number of observed absorption bands is generally lower than the total number of fundamental vibrations due to some vibration modes being inactive in the IR spectrum. Integral multiples of fundamental absorption frequencies, combinations of fundamental frequencies, and coupling interactions between fundamental vibrations generate additional bands with lower intensities than the fundamental bands. However, the combination of these factors produces a unique IR spectrum for each compound [44]. IR absorption information is presented in the form of a spectrum, with wavelength on the x-axis and absorption intensity or percent transmittance on the y-axis. Transmittance (T), the ratio of transmitted radiant power (I) to incident radiant power (I₀), defines absorbance (A) as the base-10 logarithm of the reciprocal of transmittance [44]. The IR spectral region ranges from 0.78 μm to about 1000 μm, distinguishing near-infrared (780 nm to 2.5 μm),

mid-infrared (2.5 μm to 50 μm), and far-infrared (50 μm to 1000 μm) regions. IR spectroscopy is widely used to investigate the structure of small molecules due to its sensitivity to chemical composition and molecular architecture [46]. A key advantage is its applicability to virtually any sample state with a reasonable choice of sampling technique [45]. Other advantages include high time resolution (down to 1 μs with moderate effort), low sample requirements (typically 10–100 μg), short measuring time, and relatively low costs [47]. However, some drawbacks include the lack of measurable mid-IR spectra for certain materials, increasing complexity with specimen composition, and intense peaks from liquid water potentially masking solute spectra [48]. Presently, commercially available infrared spectrometers are primarily Dispersive or Fourier Transform (FT-IR) spectrometers, with FT-IR spectrometry gaining prominence due to its ability to simultaneously examine all frequencies and analyse areas not feasible with dispersive spectrometers [44] (*Figure 16*).

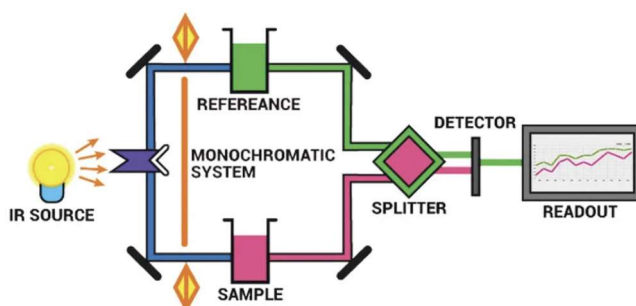


FIGURE 16 IR SPECTROSCOPY SYSTEM [58]

MATERIALS AND METHODS

The tests outlined below were conducted at the laboratories of Tiss'You SRL Regenerative Company, a firm specializing in regenerative medicine. Situated in Domagnano, a district of the Republic of San Marino, the company is dedicated to the advancement and manufacturing of biomaterials and medical devices designed to enhance the innate regenerative capacity of human body.

For this study, deantigened horse bone in the form of powder have been used. In particular, the heterologous material is employed to coat titanium implants, and it can be processed and used in two versions. The first version is the one resulting from the de-cellularization process in which are still present ECM proteins that give the powder a yellowish color (Matrix); the second version, instead, is not treated with hydrogen peroxide before the bonding treatment.

To produce the powder, the process is initiated by treating cut pieces of the aforementioned heterologous material in various shapes. Following the extraction from the original bone, the pieces underwent a washing procedure. Subsequently, they were introduced into a reactor for overnight processing, undergoing alkaline transesterification in a solution containing soda ash and methanol to eliminate lipids and cells. Products were taken out of the reactor after 15 hours reaction, washed in water to release byproducts (glycerol) and remove the solvent. Once thoroughly cleaned, samples were then placed in an oven KLARSTEIN for 24 hours at 50 degrees Celsius, a procedure referred to dehydration (*Figure 17*).



FIGURE 17 IN THE LEFT PICTURE THERE IS THE REACTOR, IN THE RIGHT ONE THERE IS THE OVEN

The dried pieces are fed into a RETSCH SK 300 for crushing, resulting in bone elements of varying grain sizes. The final stage is sieving, employing a method that utilizes specialized sieves arranged in a series, with each sieve retaining the solid fraction containing granules larger than the sieve holes. The sieve column is typically mounted on a mechanical shaker, commonly referred to as a vibrating screen [59]. The sieves come in various sizes and are stacked in a column, one atop the other. Starting from the top of the RETSCH AS 200 BASIC, the sieves are 6.3mm, followed by 4mm (with grain sizes between 4mm and 6mm utilized in orthopedic and neurological applications), 2.3mm, 1mm (with grain sizes between 1mm and 0.25mm applied in orthodontic applications), 500 micrometers, and 250 micrometers (*Figure 18*).



FIGURE 18 RETSCH SK 300 ON THE LEFT AND ON THE RIGHT

For this particular study, a minimum grain size under 250 micrometers is essential to facilitate the formation of covalent bonds between titanium and powder. To achieve this, the microgranules underwent further pulverization using a RETSCH ZM 200 pulverizer equipped with a sieve, blade, and a closed system, which serves as the recovery component (*Figure 19*).

The powder is then treated with hydrogen peroxide, 4°C at room temperature to obtain a final product containing 70% hydroxyapatite and 30% ECM (Matrix). Alternatively, a sample of intact-matrix hydroxyapatite powder was not oxidized before the bonding reaction.



FIGURE 19 RETSCH ZM 200

1. REAGENTS AND DEVICES

In the conducted experiments, the substances employed as reactants include the following (*Figure 20-21*):

- Calcium Hydroxyapatite powder of spongy bone (calcined powder - particle size < 250 μm);
- Matrix powder of spongy bone (non-calcinated powder - particle size < 250 μm);
- Hydrochloric Acid (HCl – 37% - code:18L274020);
- Acetic Acid (CH₃COOH – 96% - code:Z0492662);
- Invitrogen kit:
 - NuPAGE 4-12% Bis-Tris Gel (code:NP0322B0X);
 - PageRuler Plus Prestained Protein Ladder (code:26619);
 - NuPAGE LDS Sample Buffer (4x) (code:NP0008);
 - NuPAGE Sample Reducing Agent (10x) (code:NP0009);
 - SYPRO Ruby protein gel stain (code:S12000);
 - NuPAGE MES SDS Running Buffer (20x) (code:NP002);
- Methanol (CH₄O – 99,5% - code:TC14893QQ);
- Sulfuric Acid (H₂SO₄ – 95% - code:2878475);
- Potassium Hydroxide (KOH – 90%);

- “Acros Organics” Hydrogen Peroxide (H₂O₂ - 35 wt% - code:202460010);
- Potassium Chloride (KCl – code:102039482);
- Calcium Chloride (CaCl₂);
- Sodium Chloride (NaCl);
- Deionized water;
- Grade 6 titanium bars (Zapp precision metals GmbH);
- Grade 4 titanium screws (Clover Orthopedics SRL);
- Aluminium foil.



FIGURE 20 GRADE 6 TITANIUM BAR (ON THE TOP), GRADE 4 TITANIUM SCREW (ON THE BOTTOM)

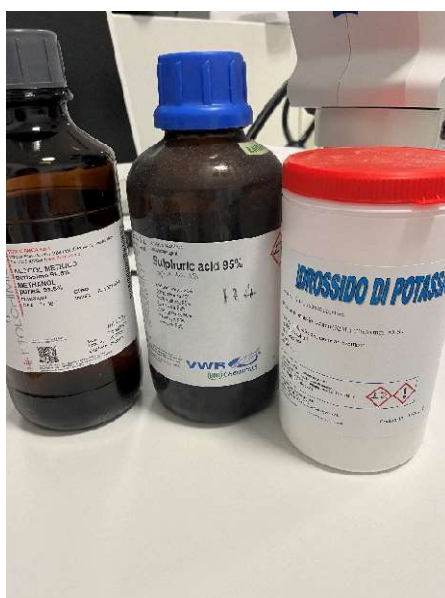


FIGURE 21 SOME OF THE REAGENTS USED

The equipment utilized includes (*Figure 22-23-24-25*):

- “Ohaus” Scout™ portable balance STX1202;
- “Ohaus” Adventurer™ Analytical balance AX124;
- “ARGO LAB” M3-D Magnetic stirrer with ceramic heating plate;
- “DK SONIC” Ultrasonic cleaner DK-80;
- “ELGA Veolia” PURELAB® Flex 3 water dispenser and deionization system;
- “Carl ZEISS microscopy GmbH” ZEISS Stemi 508 and Axiocam ERc 5s;
- “Invitrogen” iBright FL1000 Imaging Systems;
- “Ohaus” frontier 5816r;

- “Ohaus” thermal agitator for incubation and cooling;
- “PerkinElmer” FT-IR spectrometer Spectrum two;
- “Invitrogen” Mini Gel tank;
- “Life Technologies” PowerEase 300W.



FIGURE 22 SCOUT™ STX1202 (LEFT); ADVENTURER™ ANALYTICAL AX124 (RIGHT)

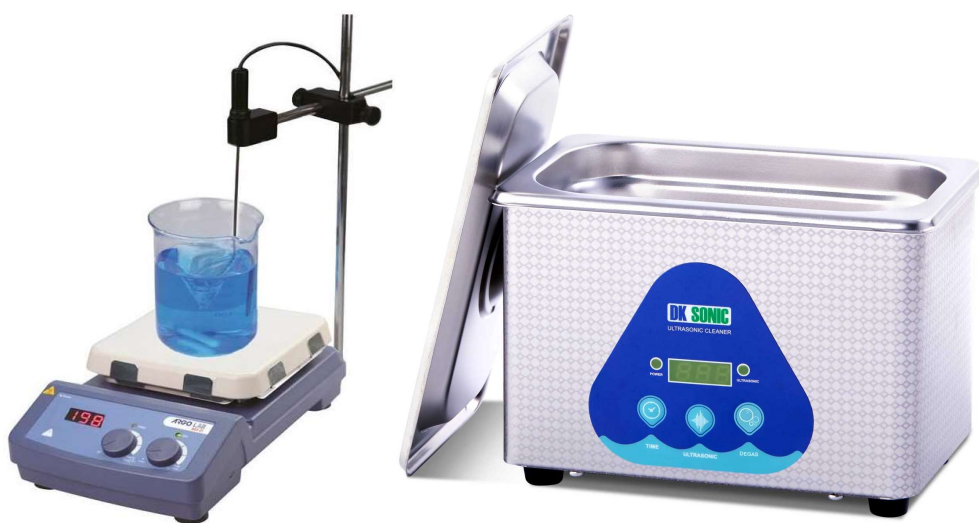


**FIGURE 23 M3-D MAGNETIC STIRRER WITH CERAMIC HEATING PLATE (LEFT);
ULTRASONIC CLEANER DK-80 (RIGHT)**



FIGURE 24 PURELAB® FLEX 3 WATER DISPENSER AND DEIONIZATION SYSTEM



FIGURE 25 ZEISS STEMI 508 (LEFT) AND AXIOCAM ERC 5S (RIGHT)

2. GENERAL PROCEDURE

Once the powder was obtained, the bars and screws were cleaned. For the cleaning, a solution of 530 microlitres of sulphuric acid in 100 microlitres of laboratory water was prepared in a beaker, the solution was then placed on a hot plate (ARGO LAB M3-D thermal plate) heated to 340 degrees Celsius and, once it reached boiling point, titanium rods and screws were placed in the mixture and left for about an hour until the surface was completely clean.

The general procedure followed for each test is the following (*Figure 26*) (*Table 1*):

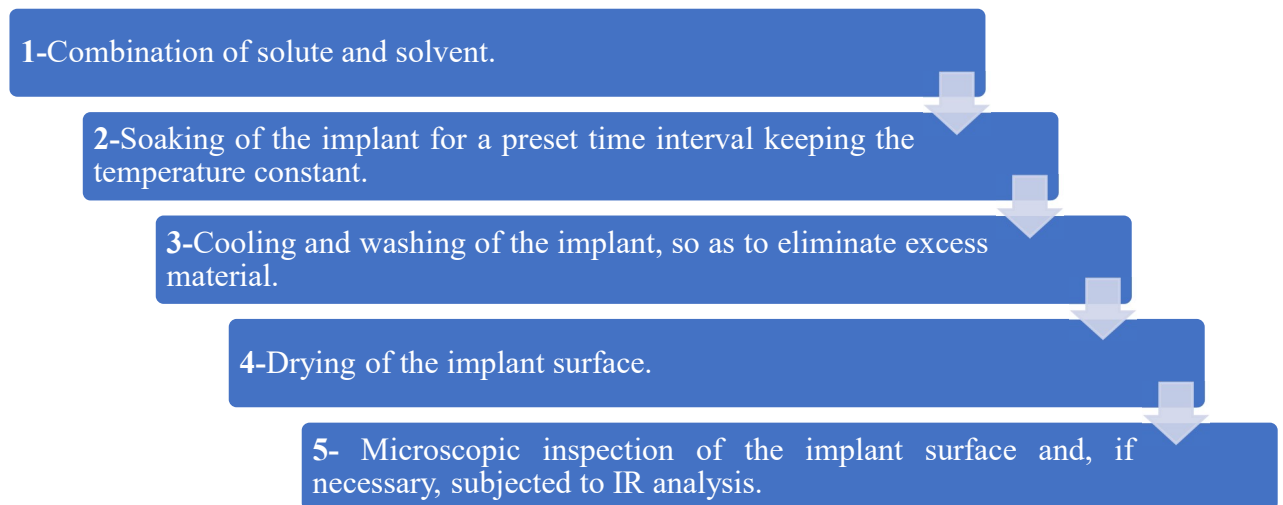


FIGURE 26 SCHEMATIC REPRESENTATION OF PASSAGES COMMON TO ALL TESTS

2.1. 1ST° TEST

- Preparation of the solution: 25 ml of hydrogen peroxide is mixed with 1,4 g of potassium hydroxide;
- The previously obtained matrix hydroxyapatite is further sieved with ASTM sieves to obtain a powder less than 150 micrometres in size;
- The powder and solution are mixed in a 6:10 ratio: 3 g of sieved powder is then mixed with 5 ml of solution;
- The titanium bar is embedded in a beaker, positioned above the heated plate;
- After approximately 10 minutes over the heat, the bar is ready and it is washed with deionised laboratory water to remove excess material. The deionised water is distilled using the PURELAB® flex 3 system;
- Drying at room temperature;
- When the implant surface is completely dry, it can be inspected under the ZEISS Stemi 508 microscope.

2.2. 2ND° TEST

- Preparation of the solution: 25 ml of hydrogen peroxide is mixed with 1,4 g of potassium hydroxide;

- The previously obtained matrix hydroxyapatite is further sieved with ASTM sieves to obtain a powder less than 150 micrometres in size;
- The powder and solution are mixed in a 6:10 ratio: 3 g of sieved powder is then mixed with 5 ml of solution;
- The titanium bar is sprinkled with compound, wrapped in aluminium foil and heated in direct contact with the hot plate;
- After approximately 10 minutes over the heat, the bar is ready and it is washed with deionised laboratory water to remove excess material;
- Drying at room temperature;
- When the implant surface is completely dry, it can be inspected under the ZEISS Stemi 508 microscope.

2.3. 3RD^o TEST

- Preparation of a more diluted solution: 25 ml of hydrogen peroxide is mixed with 2,8 g of potassium hydroxide and 25 ml of deionized water, to arrive to have total volume of 50 ml;
- The previously obtained matrix hydroxyapatite is further sieved with ASTM sieves to obtain a powder less than 150 micrometres in size;
- The powder and solution are mixed in a 6:10 ratio: 3 g of sieved powder is then mixed with 5 ml of solution;
- The titanium bar is sprinkled with compound, wrapped in aluminium foil and heated in direct contact with the hot plate;
- After approximately 10 minutes over the heat, the bar is ready and it is washed with deionised laboratory water to remove excess material;
- Drying at room temperature;
- When the implant surface is completely dry, it can be inspected under the ZEISS Stemi 508 microscope.

2.4. 4TH^o TEST

- Preparation of the solution: 25 ml of hydrogen peroxide is mixed with 1,4 g of potassium hydroxide;
- The previously obtained matrix hydroxyapatite is further sieved with ASTM sieves to obtain a powder less than 150 micrometres in size;

- The powder and solution are mixed in a 6:10 ratio: 3 g of sieved powder is then mixed with 5 ml of solution;
- The titanium bar is sprinkled with compound, wrapped in aluminium foil and heated in direct contact with the hot plate;
- After approximately 10 minutes over the heat, the bar is ready and it is washed with deionised laboratory water to remove excess material;
- The bar is left to cool inside the aluminium foil;
- When the bar has cooled down, it is washed with deionised water to remove unbound material;
- Drying on a heated plate, not at room temperature;
- When the implant surface is completely dry, it can be inspected under the ZEISS Stemi 508 microscope.

2.5. 5TH^o TEST

- Preparation of the solution: 25 ml of hydrogen peroxide is mixed with 1,4 g of potassium hydroxide;
- The previously obtained matrix hydroxyapatite is further sieved with Tivek to obtain a powder size even smaller;
- The powder and solution are mixed in a 6:10 ratio: 3 g of sieved powder is then mixed with 5 ml of solution;
- The titanium bar is sprinkled with compound, wrapped in aluminium foil and heated in direct contact with the hot plate;
- After approximately 10 minutes over the heat, the bar is ready and it is washed with deionised laboratory water to remove excess material;
- The bar is left to cool inside the aluminium foil;
- When the bar has cooled down, it is washed with deionised water to remove unbound material;
- Drying on a heated plate, not at room temperature;
- When the implant surface is completely dry, it can be inspected under the ZEISS Stemi 508 microscope.

2.6. 6TH^o TEST

- Preparation of a more diluted solution: 25 ml of hydrogen peroxide is mixed with 2,8 g of potassium hydroxide and 25 ml of deionized water, to arrive to have total volume of 50 ml;
- The previously obtained matrix hydroxyapatite is further sieved with Tivek to obtain a powder size even smaller;
- The powder and solution are mixed in a 6:10 ratio: 3 g of sieved powder is then mixed with 5 ml of solution;
- The titanium bar is sprinkled with compound, wrapped in aluminium foil and heated in direct contact with the hot plate;
- After approximately 10 minutes over the heat, the bar is ready and it is washed with deionised laboratory water to remove excess material;
- The bar is left to cool inside the aluminium foil;
- When the bar has cooled down, it is washed with deionised water to remove unbound material;
- Drying on a heated plate, not at room temperature;
- When the implant surface is completely dry, it can be inspected under the ZEISS Stemi 508 microscope.

2.7. 7TH^o TEST

- Preparation of the solution: 25 ml of hydrogen peroxide is mixed with 1,4 g of potassium hydroxide;
- The matrix powder previous obtained (the yellowest one, not treated with peroxide, not oxidised) is further sieved with Tivek to obtain a powder size even smaller;
- The powder and solution are mixed in a 6:10 ratio: 3 g of sieved powder is then mixed with 5 ml of solution;
- The titanium bar is sprinkled with compound, wrapped in aluminium foil and heated in direct contact with the hot plate;
- After approximately 10 minutes over the heat, the bar is ready and it is washed with deionised laboratory water to remove excess material;
- The bar is left to cool inside the aluminium foil;
- When the bar has cooled down, it is washed with deionised water to remove unbound material;

- Drying on a heated plate, not at room temperature;
- When the implant surface is completely dry, it can be inspected under the ZEISS Stemi 508 microscope.

2.8. 8TH^o TEST

- Preparation of the solution: 25 ml of hydrogen peroxide is mixed with 1,4 g of potassium hydroxide;
- The previously obtained matrix hydroxyapatite is further sieved with Tivek to obtain a powder size even smaller;
- The powder and solution are mixed in a 6:10 ratio: 3 g of sieved powder is then mixed with 5 ml of solution;
- The titanium bar is sprinkled with compound, wrapped in aluminium foil and heated in direct contact with the hot plate;
- After approximately 10 minutes over the heat, the bar is ready and it is washed with deionised laboratory water to remove excess material;
- The rod is left to cool inside the aluminium foil;
- When the rod has cooled down, it is washed with deionised water to remove unbound material;
- Drying on a heated plate, not at room temperature;
- Once dried, a second covering operation was carried out on the already covered surface:
 - The powder and solution are mixed in a 6:10 ratio; 3 g of sieved powder is then mixed with 5 ml of solution;
 - The titanium bar is sprinkled with compound, wrapped in aluminium foil and heated in direct contact with the hot plate;
 - After approximately 10 minutes over the heat, the bar is ready and it is washed with deionised laboratory water to remove excess material;
 - The bar is left to cool inside the aluminium foil;
 - When the bar has cooled down, it is washed with deionised water to remove unbound material;
 - Drying on a heated plate, not at room temperature;
- When the implant surface is completely dry, it can be inspected under the ZEISS Stemi 508 microscope.

2.9. 9TH° TEST

In previous experiments, it was seen that on bars with less oxide on the surface, the cover appeared more stable, so the following procedure was followed in this test:

- A solution consisting of 2,63 ml of sulphuric acid with laboratory water added, to arrive at a concentration of 1 Mol is prepared;
- The solution is heated and two titanium bars of equal size are placed in the solution until they turn dark, so that it is clear that the oxide layer on the surface has been removed;
- The now dark bars are cooled to room temperature;
- One of them, is immersed in hydrogen peroxide, so that the surface oxide layer reformed;
- At this point, you have one bar that is darker, without the oxide layer, and one that is lighter, due to the reformation of oxide on the surface;
- On both, the following procedure is then performed:
 - Preparation of the solution: 25 ml of hydrogen peroxide is mixed with 1,4 g of potassium hydroxide;
 - The previously obtained matrix hydroxyapatite is further sieved with Tivek to obtain a powder size even smaller;
 - The powder and solution are mixed in a 6:10 ratio: 3 g of sieved powder is then mixed with 5 ml of solution;
 - The titanium bar is sprinkled with compound, wrapped in aluminium foil and heated in direct contact with the hot plate;
 - After approximately 10 minutes over the heat, the bar is ready and it is washed with deionised laboratory water to remove excess material;
 - The bar is left to cool inside the aluminium foil;
 - When the bar has cooled down, it is washed with deionised water to remove unbound material;
 - Drying on a heated plate, not at room temperature;
 - When the implant surface is completely dry, it can be inspected under the ZEISS Stemi 508 microscope.

2.10. 10TH° TEST

- Preparation of the solution: 25 ml of hydrogen peroxide is mixed with 1,4 g of potassium hydroxide, 0,110 g of calcium chloride and deionized water to arrive at a concentration of 1 Mol;
- The previously obtained matrix hydroxyapatite is further sieved with Tivek to obtain a powder size even smaller;
- The powder and solution are mixed in a 6:10 ratio: 3 g of sieved powder is then mixed with 5 ml of solution;
- The titanium bar is sprinkled with compound, wrapped in aluminium foil and heated in direct contact with the hot plate;
- After approximately 10 minutes over the heat, the bar is ready and it is washed with deionised laboratory water to remove excess material;
- The bar is left to cool inside the aluminium foil;
- When the bar has cooled down, it is washed with deionised water to remove unbound material;
- Drying on a heated plate, not at room temperature;
- When the implant surface is completely dry, it can be inspected under the ZEISS Stemi 508 microscope.

2.11. 11TH° TEST

- Preparation of the solution: 25 ml of hydrogen peroxide is mixed with 1,4 g of potassium hydroxide, 0,0584 g of sodium chloride and deionized water to arrive at a concentration of 1 Mol;
- The previously obtained matrix hydroxyapatite is further sieved with Tivek to obtain a powder size even smaller;
- The powder and solution are mixed in a 6:10 ratio: 3 g of sieved powder is then mixed with 5 ml of solution;
- The titanium bar is sprinkled with compound, wrapped in aluminium foil and heated in direct contact with the hot plate;
- After approximately 10 minutes over the heat, the bar is ready and it is washed with deionised laboratory water to remove excess material;
- The bar is left to cool inside the aluminium foil;

- When the bar has cooled down, it is washed with deionised water to remove unbound material;
- Drying on a heated plate, not at room temperature;
- When the implant surface is completely dry, it can be inspected under the ZEISS Stemi 508 microscope.

2.12. 12TH° TEST

- Preparation of the solution: 25 ml of hydrogen peroxide is mixed with 1,4 g of potassium hydroxide, 0,0745 g of potassium chloride and deionized water to arrive at a concentration of 1 Mol;
- The previously obtained matrix hydroxyapatite is further sieved with Tivek to obtain a powder size even smaller;
- The powder and solution are mixed in a 6:10 ratio: 3 g of sieved powder is then mixed with 5 ml of solution;
- The titanium bar is sprinkled with compound, wrapped in aluminium foil and heated in direct contact with the hot plate;
- After approximately 10 minutes over the heat, the bar is ready and it is washed with deionised laboratory water to remove excess material;
- The bar is left to cool inside the aluminium foil;
- When the bar has cooled down, it is washed with deionised water to remove unbound material;
- Drying on a heated plate, not at room temperature;
- When the implant surface is completely dry, it can be inspected under the ZEISS Stemi 508 microscope.

2.13. 13TH° TEST

- Preparation of the solution: 25 ml of hydrogen peroxide is mixed with 1,4 g of potassium hydroxide, 0,5550 g of calcium chloride and deionized water to arrive at a concentration of 1 Mol;
- The previously obtained matrix hydroxyapatite is further sieved with Tivek to obtain a powder size even smaller;
- The powder and solution are mixed in a 6:10 ratio: 3 g of sieved powder is then mixed with 5 ml of solution;

- The titanium bar is sprinkled with compound, wrapped in aluminium foil and heated in direct contact with the hot plate;
- After approximately 10 minutes over the heat, the bar is ready and it is washed with deionised laboratory water to remove excess material;
- The bar is left to cool inside the aluminium foil;
- When the bar has cooled down, it is washed with deionised water to remove unbound material;
- Drying on a heated plate, not at room temperature;
- When the implant surface is completely dry, it can be inspected under the ZEISS Stemi 508 microscope.

2.14. 14TH° TEST

- Preparation of the solution: 25 ml of hydrogen peroxide is mixed with 1,4 g of potassium hydroxide, 0,2922 g of sodium chloride and deionized water to arrive at a concentration of 1 Mol;
- The previously obtained matrix hydroxyapatite is further sieved with Tivek to obtain a powder size even smaller;
- The powder and solution are mixed in a 6:10 ratio: 3 g of sieved powder is then mixed with 5 ml of solution;
- The titanium bar is sprinkled with compound, wrapped in aluminium foil and heated in direct contact with the hot plate;
- After approximately 10 minutes over the heat, the bar is ready and it is washed with deionised laboratory water to remove excess material;
- The bar is left to cool inside the aluminium foil;
- When the bar has cooled down, it is washed with deionised water to remove unbound material;
- Drying on a heated plate, not at room temperature;
- When the implant surface is completely dry, it can be inspected under the ZEISS Stemi 508 microscope.

2.15. 15TH° TEST

- Preparation of the solution: 25 ml of hydrogen peroxide is mixed with 1,4 g of potassium hydroxide, 0,3728 g of potassium chloride and deionized water to arrive at a concentration of 1 Mol;
- The previously obtained matrix hydroxyapatite is further sieved with Tivek to obtain a powder size even smaller;
- The powder and solution are mixed in a 6:10 ratio: 3 g of sieved powder is then mixed with 5 ml of solution;
- The titanium bar is sprinkled with compound, wrapped in aluminium foil and heated in direct contact with the hot plate;
- After approximately 10 minutes over the heat, the bar is ready and it is washed with deionised laboratory water to remove excess material;
- The bar is left to cool inside the aluminium foil;
- When the bar has cooled down, it is washed with deionised water to remove unbound material;
- Drying on a heated plate, not at room temperature;
- When the implant surface is completely dry, it can be inspected under the ZEISS Stemi 508 microscope.

2.16. 16TH° TEST

- Preparation of the solution: 25 ml of hydrogen peroxide is mixed with 1,4 g of potassium hydroxide;
- The previously obtained matrix hydroxyapatite is further sieved with Tivek to obtain a powder size even smaller;
- The powder and solution are mixed in a 6:10 ratio: 3 g of sieved powder is then mixed with 5 ml of solution;
- The titanium screw is sprinkled with compound, wrapped in aluminium foil and heated in direct contact with the hot plate;
- After approximately 10 minutes over the heat, the screw is ready and it is washed with deionised laboratory water to remove excess material;
- The screw is left to cool inside the aluminium foil;
- When the screw has cooled down, it is washed with deionised water to remove unbound material;

- Drying on a heated plate, not at room temperature;
- When the implant surface is completely dry, it can be inspected under the ZEISS Stemi 508 microscope.

2.17. 17TH° TEST

- Preparation of a more diluted solution: 25 ml of hydrogen peroxide is mixed with 2,8 g of potassium hydroxide and 25 ml of deionized water, to arrive to have total volume of 50 ml;
- The previously obtained matrix hydroxyapatite is further sieved with Tivek to obtain a powder size even smaller;
- The powder and solution are mixed in a 6:10 ratio: 3 g of sieved powder is then mixed with 5 ml of solution;
- The titanium screw is sprinkled with compound, wrapped in aluminium foil and heated in direct contact with the hot plate;
- After approximately 10 minutes over the heat, the bar is ready and it is washed with deionised laboratory water to remove excess material;
- The screw is left to cool inside the aluminium foil;
- When the screw has cooled down, it is washed with deionised water to remove unbound material;
- Drying on a heated plate, not at room temperature;
- When the implant surface is completely dry, it can be inspected under the ZEISS Stemi 508 microscope.

TABLE 1 MAIN FEATURES OF EACH TEST

TEST	POWDER	SOLUTION COMPOSITION	SIEVING METHOD	SOLUTE-SOLVENT AMOUNT	WRAPPING METHOD	DRYING TECHNIQUE	DEVICE
1	Matrix hydroxyapatite	<ul style="list-style-type: none"> • 25 ml hydrogen peroxide • 1,4 g potassium hydroxide 	ASTM	3g + 5ml	No	T amb	Bar
2	Matrix hydroxyapatite	<ul style="list-style-type: none"> • 25 ml hydrogen peroxide • 1,4 g potassium hydroxide 	ASTM	3g + 5ml	Yes	T amb	Bar
3	Matrix hydroxyapatite	<ul style="list-style-type: none"> • 25 ml hydrogen peroxide • 2,8 g potassium hydroxide 	ASTM	3g + 5ml	Yes	T amb	Bar
4	Matrix hydroxyapatite	<ul style="list-style-type: none"> • 25 ml hydrogen peroxide 	ASTM	3g + 5ml	Yes	Cooling inside the Al foil and	Bar

		<ul style="list-style-type: none"> • 1,4 g potassium hydroxide 				drying on a heated plate	
5	Matrix hydroxyapatite	<ul style="list-style-type: none"> • 25 ml hydrogen peroxide • 1,4 g potassium hydroxide 	Tyvek	3g + 5ml	Yes	Cooling inside the Al foil and drying on a heated plate	Bar
6	Matrix hydroxyapatite	<ul style="list-style-type: none"> • 25 ml hydrogen peroxide • 2,8 g potassium hydroxide • 25 ml deionized water 	Tyvek	3g + 5ml	Yes	Cooling inside the Al foil and drying on a heated plate	Bar
7	not oxidised	<ul style="list-style-type: none"> • 25 ml hydrogen peroxide • 1,4 g potassium hydroxide 	Tyvek	3g + 5ml	Yes	Cooling inside the Al foil and drying on a heated plate	Bar
8 (repeated twice)	Matrix hydroxyapatite	<ul style="list-style-type: none"> • 25 ml hydrogen peroxide • 1,4 g potassium hydroxide 	Tyvek	3g + 5ml	Yes	Cooling inside the Al foil and drying on a heated plate	Bar
9 (oxide layer removed)	Matrix hydroxyapatite	<ul style="list-style-type: none"> • 25 ml hydrogen peroxide • 1,4 g potassium hydroxide 	Tyvek	3g + 5ml	Yes	Cooling inside the Al foil and drying on a heated plate	Bar
10	Matrix hydroxyapatite	<ul style="list-style-type: none"> • 25 ml hydrogen peroxide • 1,4 g potassium hydroxide • 0,110 g calcium chloride • Deionized water to reach 1M 	Tyvek	3g + 5ml	Yes	Cooling inside the Al foil and drying on a heated plate	Bar
11	Matrix hydroxyapatite	<ul style="list-style-type: none"> • 25 ml hydrogen peroxide • 1,4 g potassium hydroxide • 0,0584 g sodium chloride • Deionized water to reach 1M 	Tyvek	3g + 5ml	Yes	Cooling inside the Al foil and drying on a heated plate	Bar
12	Matrix hydroxyapatite	<ul style="list-style-type: none"> • 25 ml hydrogen peroxide • 1,4 g potassium hydroxide • 0,0745 g potassium chloride • Deionized water to reach 1M 	Tyvek	3g + 5ml	Yes	Cooling inside the Al foil and drying on a heated plate	Bar
13	Matrix hydroxyapatite	<ul style="list-style-type: none"> • 25 ml hydrogen peroxide • 1,4 g potassium hydroxide • 0,5550 g calcium chloride • Deionized water to reach 1M 	Tyvek	3g + 5ml	Yes	Cooling inside the Al foil and drying on a heated plate	Bar
14	Matrix hydroxyapatite	<ul style="list-style-type: none"> • 25 ml hydrogen peroxide 	Tyvek	3g + 5ml	Yes	Cooling inside the Al foil and	Bar

		<ul style="list-style-type: none"> • 1,4 g potassium hydroxide • 0,2922 g sodium chloride • Deionized water to reach 1M 				drying on a heated plate	
15	Matrix hydroxyapatite	<ul style="list-style-type: none"> • 25 ml hydrogen peroxide • 1,4 g potassium hydroxide • 0,3728 g potassium chloride • Deionized water to reach 1M 	Tyvek	3g + 5ml	Yes	Cooling inside the Al foil and drying on a heated plate	Bar
16	Matrix hydroxyapatite	<ul style="list-style-type: none"> • 25 ml hydrogen peroxide • 1,4 g potassium hydroxide 	Tyvek	3g + 5ml	Yes	Cooling inside the Al foil and drying on a heated plate	Screw
17	Matrix hydroxyapatite	<ul style="list-style-type: none"> • 25 ml hydrogen peroxide • 2,8 g potassium hydroxide 	Tyvek	3g + 5ml	Yes	Cooling inside the Al foil and drying on a heated plate	Screw

3. IR-SPECTROSCOPY

The infrared spectrometer employed for analyzing the most promising samples is the FT-IR Spectrum Two spectrometer by PerkinElmer®. This instrument features a low-maintenance optical system, ensuring precise and consistent measurements day after day (*Table 2*). The proven design of the interferometer contributes to unparalleled reliability. The robust construction and integrated sampling capabilities enable analyses of raw materials in warehouse environments globally, eliminating the necessity to dispatch samples for analysis [60].

TABLE 2 MAIN CHARACTERISTICS OF SPECTRUM TWO

<i>RELEVANT TECHNICAL DATA OF SPECTRUM TWO</i>	
<i>Detector Type</i>	LiTaO ₃
<i>Operating range</i>	5 – 45°C
<i>Wavelength range</i>	8300 – 350 cm ⁻¹

The UATR (Universal Attenuated Total Reflectance Accessory) is an internal reflection device designed to simplify the analysis of solids, powders, pastes, gels, and liquids. In this technique, the sample is positioned on a crystal with a high refractive index. An infrared beam emitted by the instrument is directed into the accessory, traveling up into the crystal. It undergoes internal

reflection within the crystal, redirecting towards the detector housed in the instrument. As the beam reflects within the crystal, it penetrates the sample to a depth of a few microns (*Figure 27*).

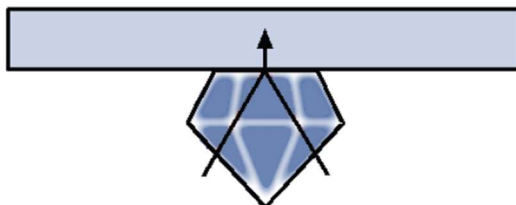


FIGURE 27 PRINCIPLE OF UATR OPERATION [61]

UATR is suitable for studying homogeneous solid samples, solid surfaces, or coatings on solid samples, ensuring good contact through applied force on the sample. The Spectrum Two UATR employs a diamond crystal known for its hardness, resistance to strong acids and bases, and high-pressure durability. Additionally, the diamond surface is not easily scratched. Although there is reduced sensitivity in the approximate range of 1900-2700 cm^{-1} , the diamond-coated UATR provides an effective scanning range that corresponds to the entire instrument range [61].

Spectrum Two incorporates numerous features enabling infrared analysis beyond the confines of the laboratory. Various power options offer the flexibility to use Spectrum Two with or without external power. Upon activation, rapid heating enables swift measurements, and optional wireless connectivity provides the convenience of portable PC control (*Figure 28*). To streamline the analytical process and enhance user experience, the comprehensive Spectrum 10™ software suite is employed. This all-encompassing FT-IR software package facilitates seamless data collection, processing, and report generation [62] (*Figure 29*).



FIGURE 28 SPECTRUM TWO FT-IR WITH UNIVERSAL ATR ACCESSORY [62]

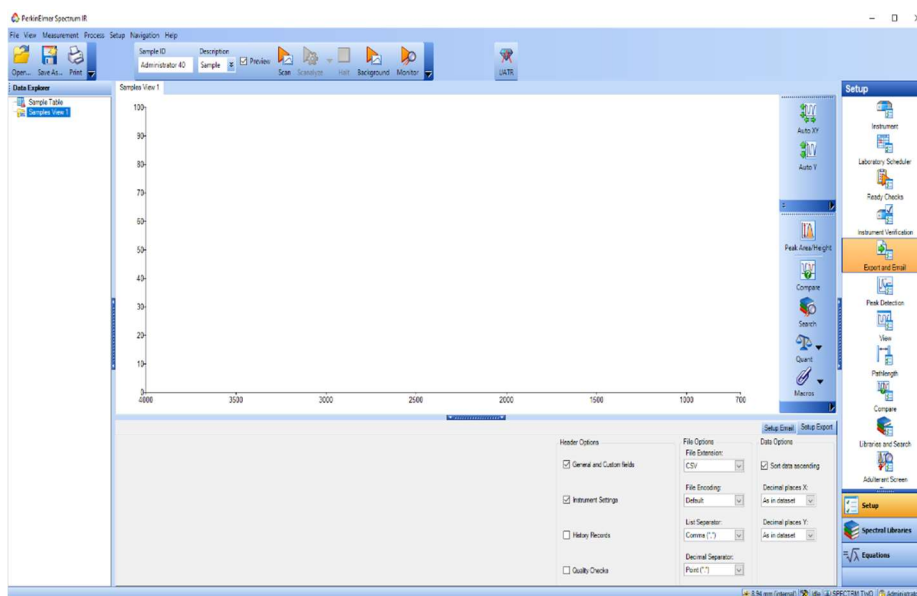


FIGURE 29 SPECTRUM 10 SOFTWARE SUITE (PERKINELMER)

3.2. PROTOCOL OF ANALYSIS

The procedure for acquiring spectra begins with launching the "PerkinElmer Spectrum IR" software. Prior to analyzing a sample, it is essential to clean the UATR module's sampling plate, achieved by using a cloth soaked in acetone. A brief wait of a few seconds ensures the plate is thoroughly dry, clean, and ready for the procedure.

The initial step involves obtaining a background scan by selecting the "Background" button on the Measurement bar. Following a brief display of the background spectrum, the Viewing Area is set up for data collection from the sample. A unique identifier is assigned to each sample by entering it in the space designated as "Sample ID."

Subsequently, the treated titanium implant is positioned on the diamond crystal within the UATR module. The spectrometer arm is temporarily halted above the crystal, initially positioned over it and then rotated clockwise until the metal tip is in proximity to the plate. Scanning is initiated by clicking the "Scan" button on the Measurement bar. The software generates a preview of the spectrum, and with another click on "Scan" within a few seconds, the actual spectrum of the sample is provided. Additionally, the "Labels" option on the lateral toolbar can be selected to assign wave numbers to the major peaks before printing the spectrum. The procedure for obtaining the spectra starts by starting the software "PerkinElmer Spectrum IR". Before starting the analysis of a sample, it is necessary to clean the sampling plate of the UATR module and it can be done using a cloth soaked in acetone; for the plate to be completely dry, clean, and ready for the procedure a few seconds are needed.

The schematic representation of the IR-analysis protocol is the following (*Figure 30*):

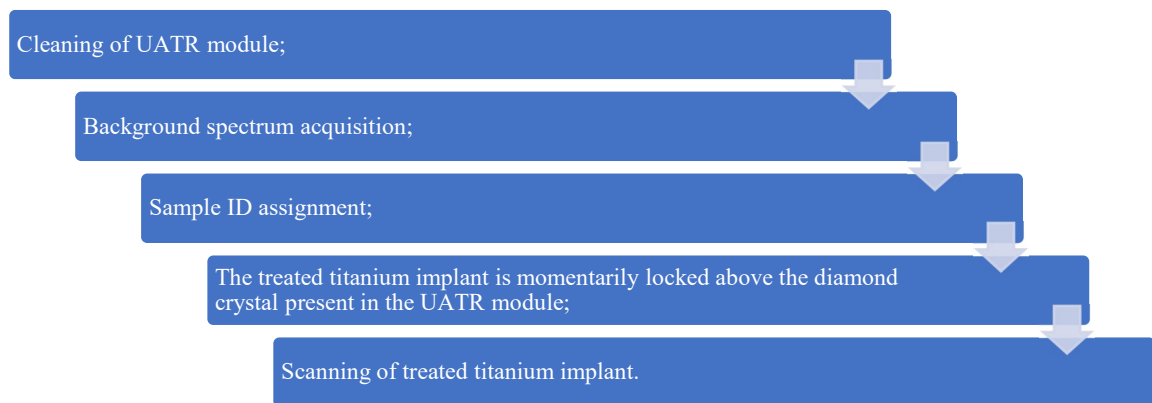


FIGURE 30 SCHEMATIC REPRESENTATION OF THE IR-ANALYSIS PROTOCOL

4. SDS PAGE

This technique is used for the qualitative analysis of protein mixtures on two samples, the matrix hydroxyapatite and the material that is attached and bound to the implant, specifically the material bound to the bar from the experiment 5. The sample related to the powder is called P, the one related to the material bound is denoted as M.

SDS PAGE technique is performed as follow:

I. DEMINERALIZATION PHASE:

This step is conducted in order to remove the ions, to extract and solubilize the collagen.

- For the hydroxyapatite powder (P), it is prepared a solution of 2,7 ml of deionized water, 200 ml of hydrochloric acid, in which 0,1 g of powder is dissolved;
- For the material attached to the bar (M), that is carefully scraped off from the bar, it is prepared a solution of 1,4 ml of deionized water, 100 ml of hydrochloric acid, in which 0,05 g of material is dissolved.

Solution and materials are placed in small test tubes and shaken in an Ohaus shaker for a few hours to promote mineral removal.

After shaking, the remaining solution containing salts must be removed, so six rinses are carried out using an orbital centrifuge. For both tubes, the liquid, taking care not to lose any material, is removed, and laboratory water is added to the tube, now containing only material. At this point, the test tubes and counter tubes (tubes with the same weight

as the two tubes containing material, used to balance the weight in the machine) are inserted into Ohaus frontier 5816r and spin for 10 minutes at 4500 rpm. This process is repeated 6 times.

II. EXTRACTION PHASE:

- Preparation of a solution 0,1 M containing 60 microliters of acetic acid and 10 ml of deionized water;
- Add 200 microliters of solution in the tube powder sample;
- Add 100 microliters of solution in the tube material sample.

The test tubes are placed in the Ohaus thermal agitator and the solution is left overnight (*Figure 31*).



FIGURE 31 TEST TUBES WITH P AND M SAMPLES READY TO BE PLACED IN THE SHAKER

III. DENATURATION PHASE:

A solution of 20 microliters is prepared. The latter is made of:

- 2 microliters of DDT (reducing agent);
- 18 microliters of sample. In the preparation of this, two different samples were prepared, A and B, which differ in the amounts of reagents and material used.

SAMPLE A: 1 microliter of material (P or M) is added to 12 microliters of deionized water and 5 microliters of LDS Sample Buffer 4x.

SAMPLE B: 3 microliter of material (P or M) is added to 10 microliters of deionized water and 5 microliters of LDS Sample Buffer 4x.

In total, at the end of the process, 4 test tubes have been set: two samples A and B for M and two samples A and B for P (*Figure 32*).



FIGURE 32 SAMPLE M: A AND B IN THE ROW ABOVE AND SAMPLE M: A AND B IN THE ROW BELOW

All the tubes are first shaken at 500 rpm for 30 minutes and then centrifuged at 16000 rpm for 10 minutes.

IV. LOADING AND RUNNING PHASE:

This is the stage that involves preparing the Invitrogen Mini Gel tank and inserting the special gel, on which the protein run will take place after the small chambers, where the gel will be inserted, will be positioned.

Initially, the Running Buffer is formulated by amalgamating 50 ml of NuPAGE MES SDS Running Buffer (20x) with an equal volume of water. Subsequently, the NuPAGE 4-12% Bis-Tris Gel is extracted from its packaging, the protective tape is removed from the lower edge, and it is positioned within one of the two chambers. Once correctly situated, the gel is inundated with Running Buffer up to its upper extremity, as denoted by a delineating line. The well protector is then disengaged, and using a pipette, liquid is introduced into each well. In the leftmost well, 5 microliters of PageRuler Plus Prestained Protein Ladder, serving as our prestained protein markers, are dispensed. Progressing from left to right, 10 microliters of each sample (PA, PB, MA, MB) are sequentially added.

Following this preparation, the loading phase commences, during which the Life Technologies PowerEase 300W is activated in a constant mode at 300 W, 20 V for a duration of 45 minutes. This establishes the requisite voltage for initiating the electrophoretic run (*Figure 33*).

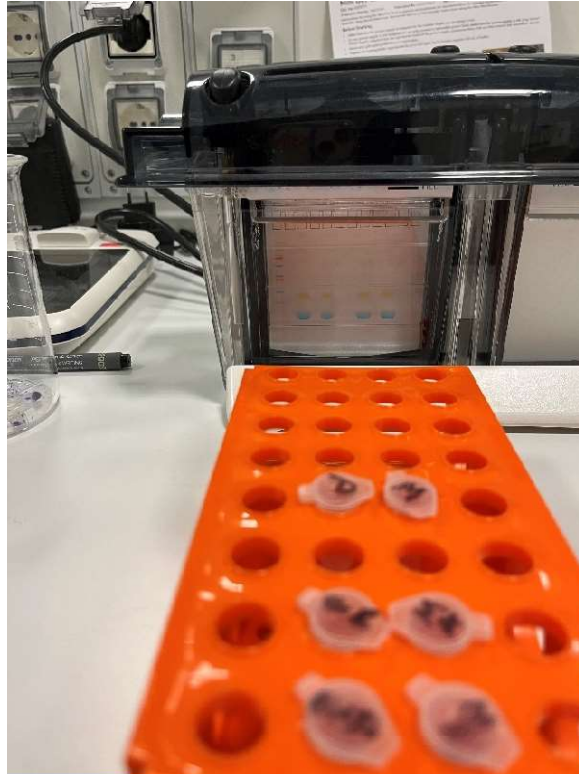


FIGURE 33 RUNNING PHASE (PROTEINS SEPARATION)

V. **FIXING PHASE:**

200 ml of a solution containing 50% of methanol, corresponding to 100 ml, and 7% of acetic acid, corresponding to 14 ml, and deionized water is prepared.

The 200 ml of solution is divided into 100 ml each, allowing for two washes. After the electrophoretic run is completed, the gel is taken from the Invitrogen Mini Gel tank and placed in a small container containing the first 100 ml of the freshly prepared solution, ensuring that the gel is completely covered by the liquid. This immersive process lasts for a few hours, after which the second wash is performed using the remaining 100 ml. After the second time, during which the gel remains in the liquid for about 30 minutes, it becomes apparent that the gel has decreased in size. Subsequently, the solution is removed, and the gel is left in water for a few minutes to allow it to rehydrate.

VI. **STAINING PHASE:** gel is left overnight in 100 ml of SYPRO Ruby protein gel stain.

VII. WASHING PHASE:

Prepare 200 ml of solution containing 10% of methanol, corresponding to 20 ml, and 7% of acetic acid, corresponding to 14 ml, and the remaining part is filled with deionized water.

The 200 ml of solution are divided into 100 ml each, allowing for two washes. Two immersions of the gel are conducted, each in 100 ml for a duration of 30 minutes.

VIII. ACQUISITION PHASE:

The acquisition is carried out using the Invitrogen iBright FL1000 Imaging System. It has a cassette that is cleaned before placing the gel. Upon activation, the PROTEIN FLUORESCENCE and PROTEIN GEL analysis options are selected for this procedure. By adjusting the exposure time, the different arrangement of proteins in the samples becomes visible. These can then be compared with the markers to draw conclusions from the analysis.

RESULTS

1. SURFACE INSPECTION

The tests described in the Materials and Methods section were listed in chronological order. This means that each subsequent test, following the previous one, was conducted in relation to the results of the preceding test, with some changes made to the process. The photographs were taken via the AxioCam ERc 5s camera, integrated into the ZEISS Stemi 508 microscope, and saved to a removable memory from which they were then recovered.

The difference between the first and second tests lies in the fact that, in the second test, the titanium bar is enclosed in a tightly sealed aluminum foil. Inside this foil, the solution with the bone powder is poured and then heated. As a result of the second experiment, a more homogeneous coverage was obtained. For this reason, the "wrapping technique" of enclosing the implant in aluminum and then pouring will be consistently employed in subsequent tests (*Figure 34*).

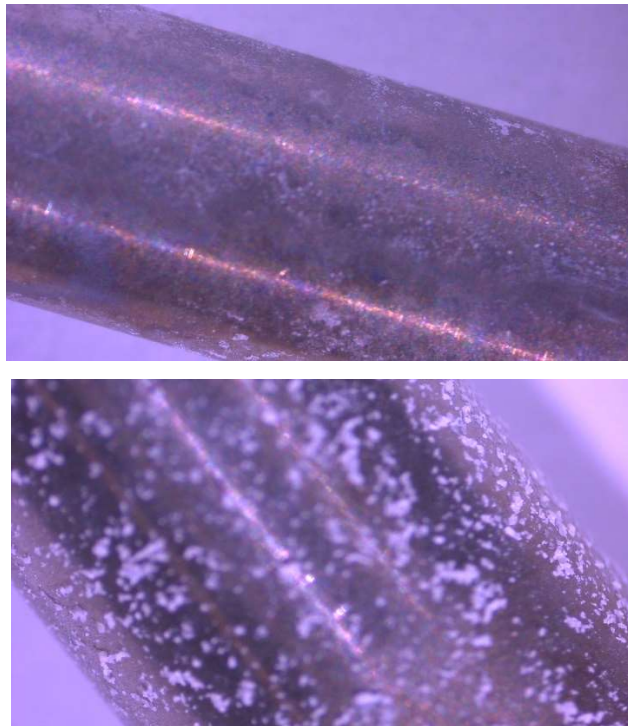


FIGURE 34 RESULT OF THE 1° TEST (ON THE LEFT) AND RESULT OF THE 2° TEST (ON THE RIGHT)

With the third test, a more diluted solution, composed by 25 ml of hydrogen peroxide is mixed with 2,8 g of potassium hydroxide and 25 ml of deionized water, to arrive to have total volume of 50 ml, was prepared. However, it was observed that upon scratching, the material on the bar was removed. Consequently, the idea of dilution was abandoned, and subsequent experiments were conducted using the previous concentration (6% potassium hydroxide in hydrogen peroxide) (*Figure 35*).



FIGURE 35 RESULT OF THE 3° TEST

With the fourth test, the results significantly improved compared to the previous tests. It was observed that, with a solution composed by 25 ml of hydrogen peroxide and 1,4 g of potassium hydroxide, if the titanium bar is left to cool inside the aluminium foil and then dried on a heated plate (rather than at room temperature), the coverage is noticeably more stable and robust. The coverage was good but not optimal. Therefore, based on the results obtained, in the fifth experiment, a filtration using a Tyvek sieve was applied to achieve a finer powder granularity. As seen in the photos, the coverage appears more homogeneous (*Figure 36*). For this reason, in subsequent experiments, the filtration using Tyvek will continue to be employed.



FIGURE 36 RESULT OF THE 4° TEST (ON THE LEFT) AND RESULT OF THE 5° TEST (ON THE RIGHT)

For the sixth test, a more diluted solution composed by 25 ml of hydrogen peroxide, mixed with 2,8 g of potassium hydroxide and 25 ml of deionized water, to arrive to have total volume of 50 ml, was prepared, while still following the considerations of the "wrapping method" and drying the bar in aluminium followed by further drying on a heated plate. However, the bar, after completing the procedure, exhibited a weaker coverage that could be easily removed by scratching, similar to previous instances (*Figure 37*). After this test, the idea of using a more diluted solution was completely abandoned.

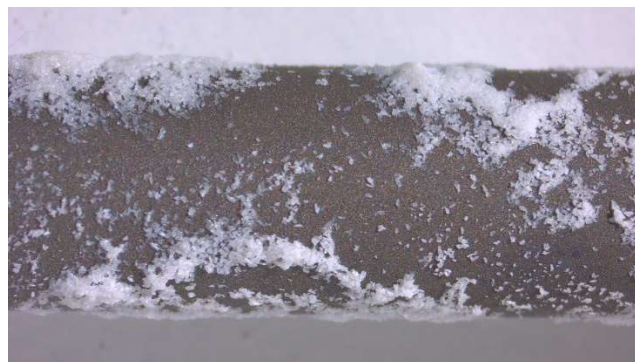


FIGURE 37 RESULT OF THE 6° TEST

For the seventh test, the STD (standard) procedure was used, following the protocol indicated in the table in the Materials and Methods section, under the name of test 5, and, instead of using matrix hydroxyapatite, matrix powder not previously oxidized was employed. Even though the coverage appears good at first glance, it can be easily removed by scratching, the resulting coverage was less robust (*Figure 38*).



FIGURE 38 RESULT OF THE 7° TEST

In the eighth experiment, the STD procedure, related to the test 5 in the table in the Materials and Methods section, was employed with matrix hydroxyapatite powder, but the procedure was applied twice to the same bar, resulting in a double coating. It was observed that, somehow, conducting a second process on the first seemed to weaken the bonds formed in the initial coating. As a result, the final coverage appeared weak and non-uniform (*Figure 39*).

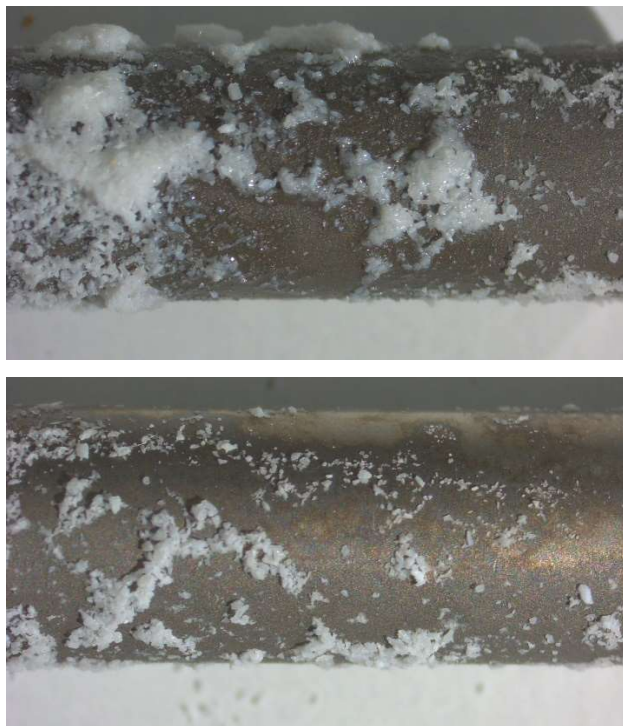


FIGURE 39 RESULTS OF THE 8° TEST

The results of the ninth test lead to a nearly uniform and stable coverage for both bars. However, for the darker one, without an oxide layer, the coverage is slightly better (*Figure 40*).



FIGURE 40 RESULT OF THE 9° TEST: COATING SHOWN OVER THE BAR WITHOUT OXIDE LAYER (ON THE LEFT) AND COATING SHOWN OVER THE BAR WITH THE OXIDE LAYER (ON THE RIGHT)

In experiments ten, eleven, and twelve, the STD procedure was followed with the addition of a calculated amount of salts, such as CaCl_2 , NaCl , and KCl , in solution. It was decided to introduce different ionic species into the reaction environment, such as K^+ , Na^+ and Ca^{2+} because it was thought that they could change the ionic balance of the system, amplifying the reaction efficiency. It was observed that the coverage is less homogeneous compared to previous tests (*Figure 41*). Therefore, in experiments thirteen, fourteen, and fifteen, the salt concentration was increased from 0.01 mol to 0.05 mol. The final coverage is slightly better than that obtained in tests ten, eleven, and twelve, but not superior to the coverage achieved in previous tests (*Figure 42*). As a result, the idea of adding additional salts was abandoned.

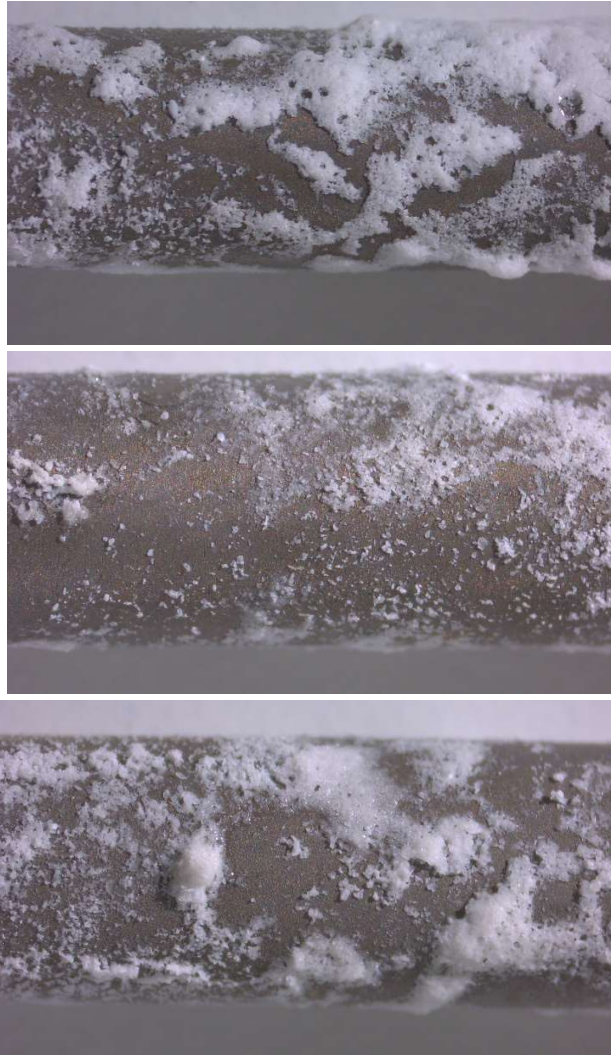


FIGURE 41 RESULT OF THE 10° TEST (ON THE LEFT-UP), RESULT OF THE 11° TEST (ON THE RIGHT-UP) AND RESULT OF THE 12° TEST (DOWN)

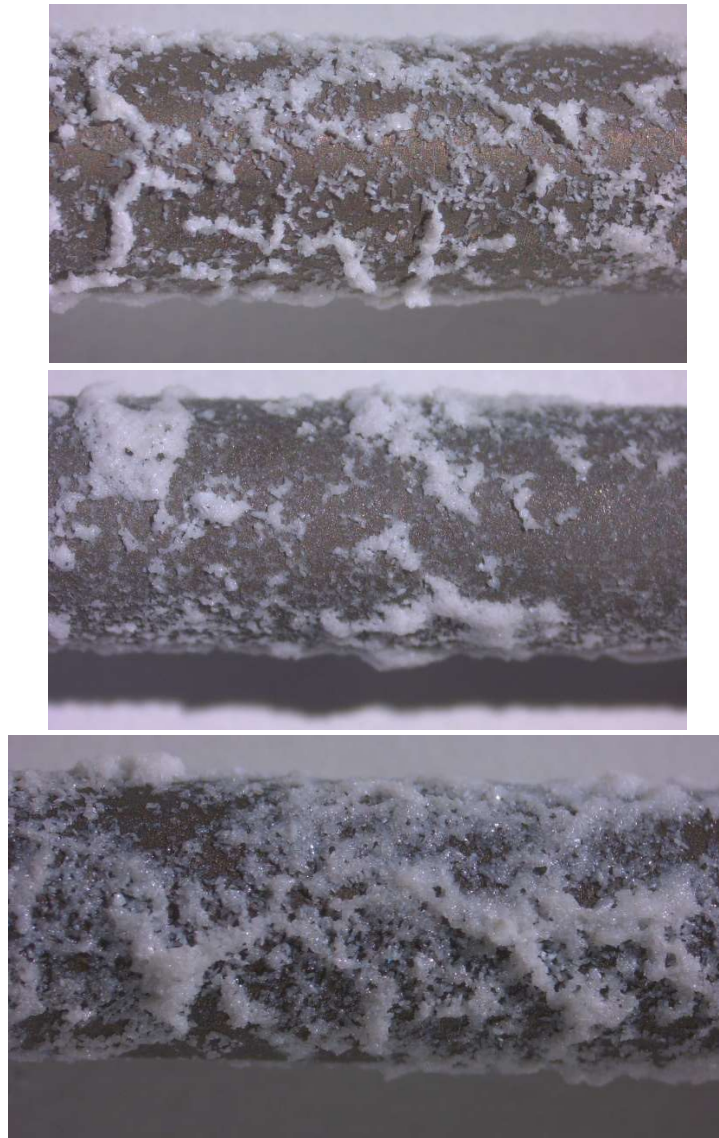


FIGURE 42 RESULT OF THE 13° TEST (ON THE LEFT-UP), RESULT OF THE 14° TEST (ON THE RIGHT-UP) AND RESULT OF THE 15° TEST (DOWN)

In tests sixteen and seventeen, the experiments conducted with the STD procedure in the fifth and sixth tests were repeated on titanium screws instead of bars. The procedure of the fifth and sixth tests are listed in the table in the Materials and Methods section, under the column "tests" with entries 5 and 6. It was observed that experiment sixteen, involving the standard procedure on screws, resulted in a more uniform and durable coverage compared to that obtained in experiment seventeen. In the latter, a thin layer of hydroxyapatite was formed, resulting in a slightly opaque white veil across the entire surface, representing an optimal coverage of the implant, even though no visible clumps were present (*Figure 43*).



FIGURE 43 RESULT OF THE 16° TEST (ON THE LEFT) AND RESULT OF THE 17° TEST (ON THE RIGHT)

2. IR- ANALYSIS

The IR analysis was performed only for titanium implants that, on surface inspection under the microscope, showed a visible layer of residual cover after treatment. The IR spectra obtained are shown below; the x-axis shows the wavenumbers of the vibration frequencies, while the y-axis shows the percentage of transmittance.

The graph below shows the IR spectra obtained in the case of the presence of alkaline substance in the coating compound. Specifically, the hydroxyapatite-based coating on the bar from the 4° test, the hydroxyapatite-based coating on the bar from the 5° test, the hydroxyapatite-based double coating on the bar from the 8° and the hydroxyapatite-based coating on the bar with the oxide layer from the 9° test (*Figure 44-45-46-47*).

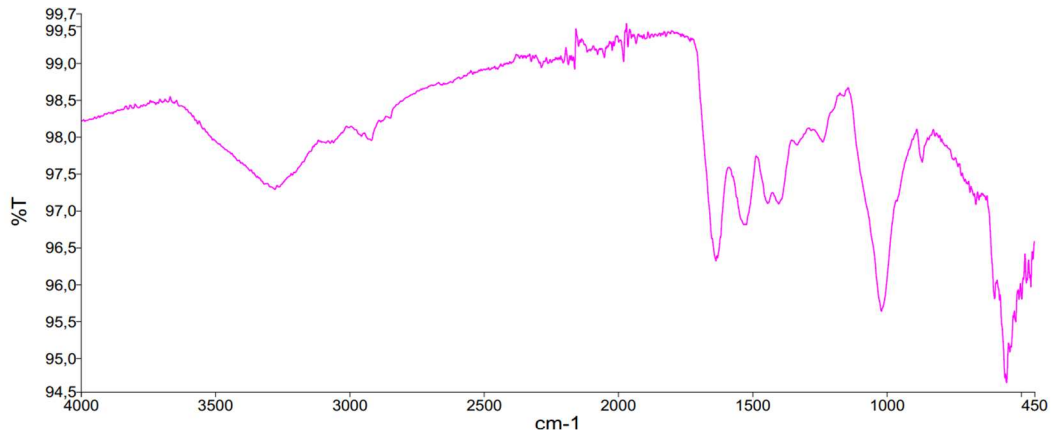


FIGURE 44 HYDROXYAPATITE-BASED COATING ON THE BAR FROM THE 4° TEST

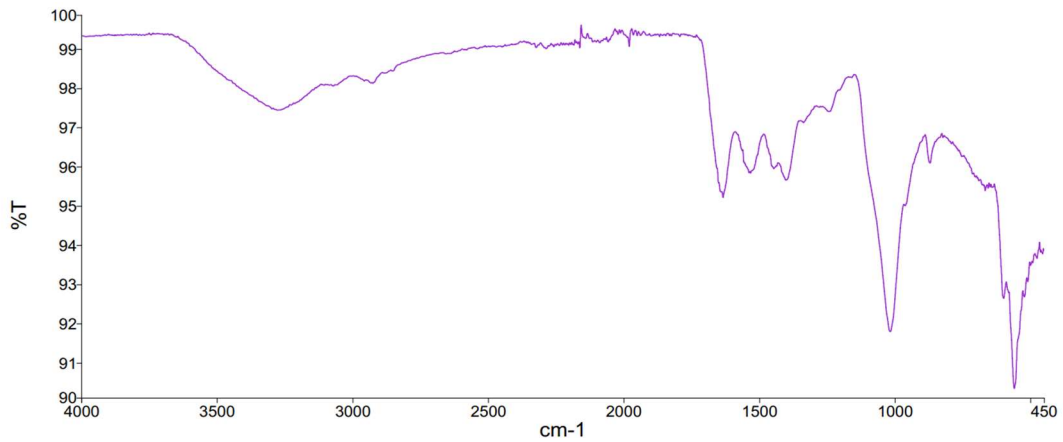


FIGURE 45 HYDROXYAPATITE-BASED COATING ON THE BAR FROM THE 5° TEST

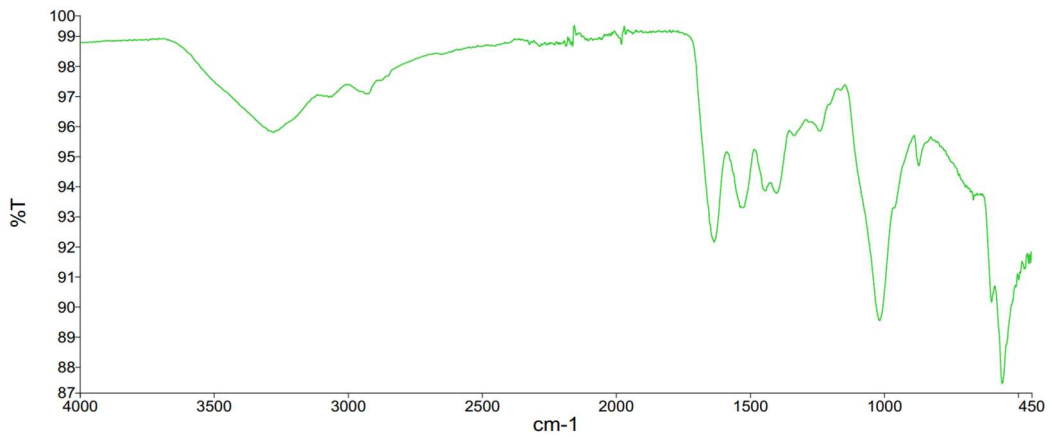


FIGURE 46 HYDROXYAPATITE-BASED DOUBLE COATING ON THE BAR FROM THE 8°

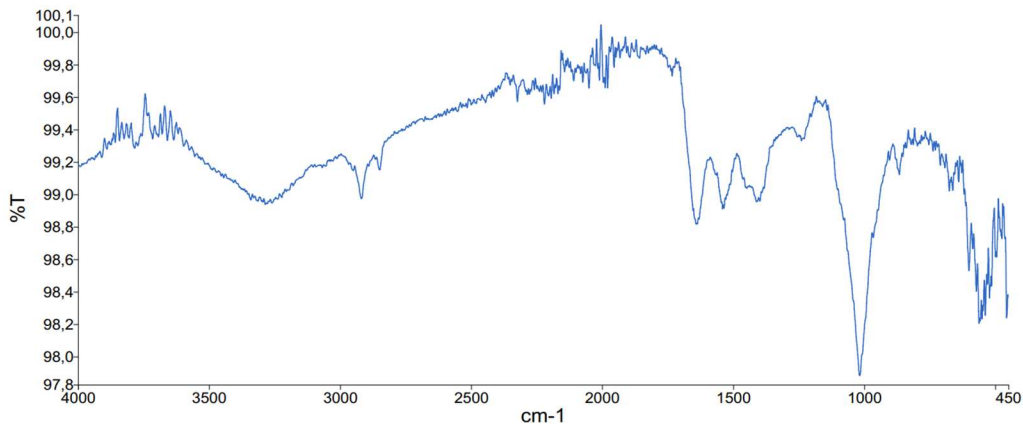


FIGURE 47 HYDROXYAPATITE-BASED COATING ON THE BAR WITH THE OXIDE LAYER FROM THE 9° TEST

Amide I, the peak around 1600 cm^{-1} , Amide II, the peak between 1470 and 1570 cm^{-1} and Amide III, the peak between 1250 and 1350 cm^{-1} are the bond resonances visible in all spectra and with the classic ratio of molar extinction coefficients typical of native proteins, demonstrating that the process does not denature the collagen contained in the intact matrix bone powder.

3. SDS PAGE

The sample related to the powder is called P, the one related to the material bound is denoted as M, from which respectively sample A and B were then prepared for both, the technique of which is indicated in section 4 on SDS PAGE in the Materials and Methods section.

In the figures below (*Figure 48*), the marker index is compared with the fluorescence gel photograph, coming from Invitrogen iBright FL1000 Imaging Systems, in which, from the left, the markers, sample PA (powder A), PB (powder B), MA (material A) and MB (material B) are visible. "Material" refers to the compound bonded and solidified on the surface of the titanium implant as a result of the 5th test. For both samples P and M, bands at 129 and 139 kDa are evident, representing the $\alpha 1$ and $\alpha 2$ chains of collagen type 1. Type I collagen is composed of three polypeptide chains, two of which are called $\alpha 1$ and $\alpha 2$. Its distinctive structure is characterised by a triple helix, in which three polypeptide chains intertwine to form a spiral structure. The formation of this triple helix is crucial for the structural and mechanical function of collagen. This conformation provides collagen with the strength and stability needed to play its supporting role in the body's connective tissues [63]. In sample M, the dimers and trimers of the molecule are also evident. Dimers and trimers represent categories of molecular aggregates consisting of two or three similar or identical molecular units, which associate

through chemical interactions. These associations may result from covalent bonds, hydrogen bonds or other forms of intermolecular interactions. Their formation can produce significant effects on the chemical and physical properties of the substances involved, as they have the potential to influence the stability, solubility, reactivity and other characteristics of the participating molecules [64].

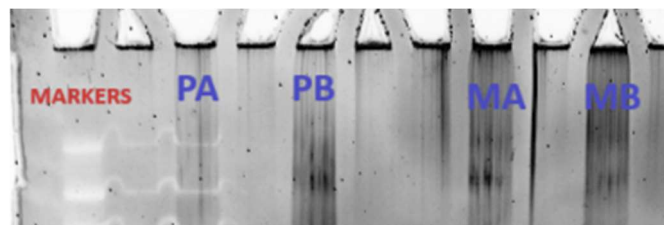


FIGURE 48 BLACK LINES AT HIGH MOLECULAR WEIGHTS SHOW DIMERS AND TRIMERS

At molecular weights between 55 and 75 kDa, possible degradation products are present in both samples, but the M sample has a component at higher molecular weights than the unbound sample (*Figure 49*). This component could therefore be attributable to a higher degradation of certain products in P than in M.

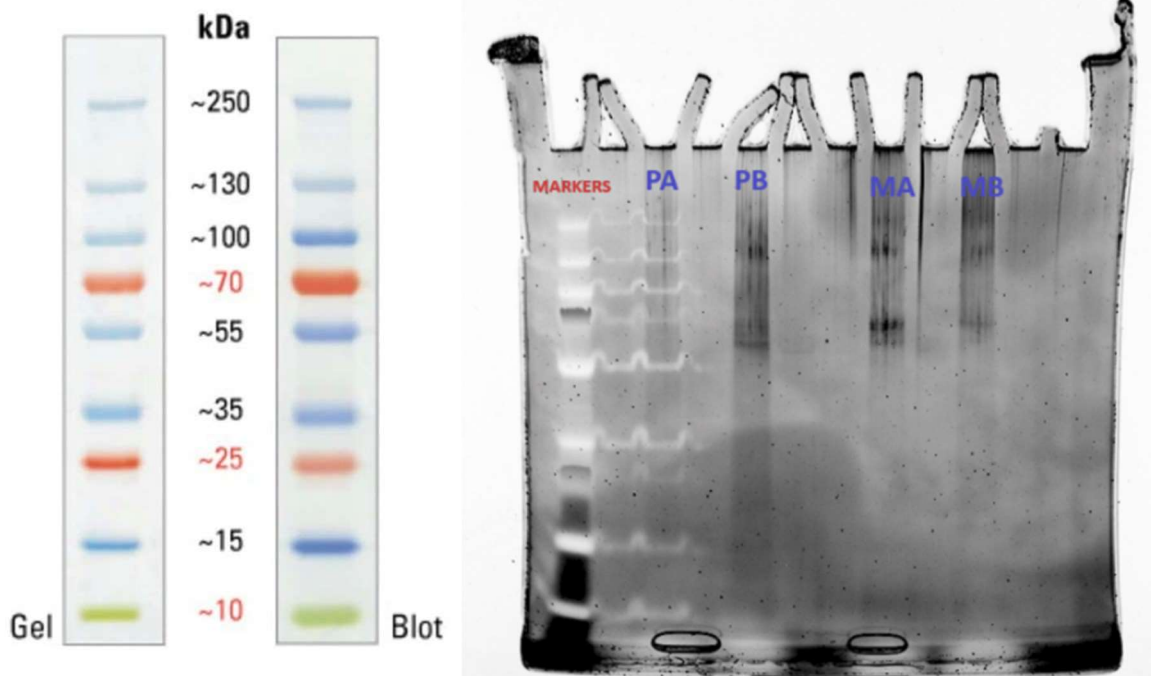


FIGURE 49 MOLECULAR WEIGHT MARKERS (ON THE LEFT) AND RESULT OF SDS PAGE (ON THE RIGHT)

DISCUSSIONS

Examining all the results obtained in various tests, also thanks to the use of photographic material, reported in the previous section, it is possible to observe that in several cases, the coverage achieved on screws and bars is uneven, especially when using more diluted solutions and when the implant is not dried on a heated plate but at room temperature. This has been shown to be a significant factor in the strong adhesion of the coating. Furthermore, under the same treatment conditions, comparing the images of Matrix-based coatings with those of Hydroxyapatite-based coatings, it is evident that Hydroxyapatite binds more easily and uniformly than Matrix. In this regard, it is possible to hypothesize, with a minimal margin of error, that the disparity between Hydroxyapatite-based coatings and Matrix-based coatings may be attributed to a higher presence of collagen in the latter. Probably, the presence of collagen in the Matrix powder reduces the possibility of contact between the oxygen atoms of the phosphate groups and those on the titanium surface, making it more difficult for bonds to form between the coating compound and the implant.

Despite these general considerations, a particular case has been identified where the coating process on the titanium implant surface proved to be more effective. This is related to the procedure carried out in the fifth test, where the best coverage result occurred when the following steps (from the Materials and Methods section) were performed (*Figure 50*):

- Preparation of the solution: 25 ml of hydrogen peroxide is mixed with 1,4 g of potassium hydroxide;
- The previously obtained matrix hydroxyapatite is further sieved with Tivek to obtain a powder size even smaller;
- The powder and solution are mixed in a 6:10 ratio: 3 g of sieved powder is then mixed with 5 ml of solution;
- The titanium bar is sprinkled with compound, wrapped in aluminium foil and heated in direct contact with the hot plate;
- After approximately 10 minutes over the heat, the bar is ready and it is washed with deionised laboratory water to remove excess material;
- The bar is left to cool inside the aluminium foil;
- When the bar has cooled down, it is washed with deionised water to remove unbound material;
- Drying on a heated plate, not at room temperature.



FIGURE 50 A HOMOGENEOUS AND STRONG RECOATING ON THE BAR, ANALYZED THROUGH A MICROSCOPE, WAS OBSERVED AFTER IT UNDERWENT THE PROCEDURE DESCRIBED IN EXPERIMENT 5

If we want to describe the decisive factors for achieving a homogeneous and resistant coating, comparing the obtained results and conducting subsequent tests based on the outcomes of those performed earlier, the following factors stand out:

- Matrix hydroxyapatite powder <250 micrometers in size;
- The use of Tyvek filter for a finer particle size. This is linked to the fact that smaller particle sizes increase the probability of contact between phosphate groups and the titanium surface, favoring the formation of a covalent bond between the hydroxyapatite powder particles;
- Preparation of the solution as described above and using a 6:10 concentration of solution and powder;
- Utilizing the "wrapping technique" and allowing it to cool inside the aluminum foil;
- Drying on a heated plate;
- It has also been observed that the coating is stronger if the implant does not have the oxide layer that titanium typically has on its surface.

Regarding the spectrum, in the ones showed in the Result section, the terms amide I, amide II, and amide III denote specific absorption patterns associated with the vibrations of amide bonds within a molecule. These distinctive amide peaks typically manifest in a particular segment of the IR spectrum, serving as indicators of the presence of amide functional groups in a given molecule.

Amide I: Pertains to the stretching vibration of the C=O (carbon-oxygen) bond and the N-H (nitrogen-hydrogen) bond in amides, typically occurring within the range of 1600-1700 cm^{-1} .

Amide II: Correlates with the bending vibrations of the N-H bond in amides, with the amide 2 peak usually falling between 1470 and 1570 cm^{-1} .

Amide III: Primarily involves the deformation vibrations of the C-N and N-H bonds in amides, typically situated in the region between 1250 and 1350 cm^{-1} .

Consistent amide I, II, and III peaks in the IR spectrum suggest that the molecular structure containing these amide functional groups is likely stable, undergoing minimal changes. This observation can be valuable for confirming the presence of specific functional groups in molecules during spectroscopic analysis.

The last procedure carried out is SDS-PAGE. In both samples (P powder and material attached to bar M), bands at 129 and 139 kDa are evident, representing the presence of alpha 1 and alpha 2 chains of type 1 collagen. This indicates that the structure of both P and M collagen is intact and correctly assembled with its two main subunits. This structural integrity is crucial for the function of collagen in providing support and resistance to the body's tissues. The presence of dimers and trimers is also important, as they provide greater structural stability compared to individual monomers. At molecular weights between 55 and 75 kDa, a higher degradation of P components compared to M is noticeable. This is an interesting aspect to emphasize. The reason why a sample of bone powder (matrix hydroxyapatite) binding to titanium may exhibit lower degradation could be attributed to various factors. The formation of a stable bond between hydroxyapatite and titanium can positively influence the material's durability. Some possible reasons might be attributed to titanium itself, for example. This metal, known for its biocompatibility and corrosion resistance, could stabilize the material and promote the formation of a strong bond between titanium and hydroxyapatite. This can influence the protection of the material from external agents, thereby contributing to its chemical stability. Additionally, the compatibility between hydroxyapatite and titanium may contribute to the structural stability of the sample, forming a solid bond that can prevent the breakage or detachment of hydroxyapatite particles, thus maintaining the material's integrity.

CONCLUSIONS

After several tests, the ultimate goal of achieving strong and homogeneous coverage on the titanium implant was achieved by combining precise factors. With the help of photographic material, it was seen that the best coverings resulted when matrix hydroxyapatite was used, instead of matrix without preoxydation protocol, appropriately filtered with a Tyvek filter. It has been hypothesised that the reason for this difference in bonding between the two powders is due the presence of multiple oxidizing radical species in the matrix hydroxyapatite powder, and therefore the oxygen of phosphates of hydroxyapatite binds more easily and more homogeneously than the matrix not treated with H₂O₂. Other important factors were dilution in hydrogen peroxide at a ratio of 6:10, in an alkaline solution obtained from the combination of hydrogen peroxide and potassium hydroxide, drying on a heated plate and the use of the wrapping method. In these cases, a visual inspection of the implant surface using a stereomicroscope showed good homogeneity of coverage. What was seen under the microscope was confirmed by the IR analysis of the samples, which revealed the presence of the coating on the surface of the titanium implant by detecting the presence of the chemical functional groups characteristic of the two powders, namely amide I, amide II and amide III. This fact is particularly significant as it allows us to conclude that, although the conditions used are different, the molecular structure containing these amide functional groups, in particular collagen, is stable, undergoing minimal changes, and the coating process developed is able to achieve the coating on the implant while maintaining the chemical properties of the material bonded to its surface. What was deduced from the IR inspection was then confirmed by the results from the SDS PAGE, it is clearly visible that the collagen chain has not been broken. The coating process therefore does not change the chemical properties of the powder used and guarantees a strong and homogenous cover, which in the long term can prevent the breakage or detachment of hydroxyapatite particles, thus maintaining the material's integrity.

REFERENCES

- [1] Wisil Dent. (2019, marzo 28). Titanio in odontoiatria [online]. Available: <https://www.wisident.it/2019/03/28/titanio-odontoiatria/>
- [2] Freese, H. L., Volas, M. G., & Wood, J. R. (2001). Metallurgy and technological properties of titanium and titanium alloys. *Titanium in Medicine, 1*.
- [3] Zhang, L. C., & Chen, L. Y. (2019). A review on biomedical titanium alloys: recent progress and prospect. *Advanced engineering materials, 21*(4), 1801215.
- [4] Ahmed, Y. M., Sahari, K. S. M., Ishak, M., & Khidhir, B. A. (2014). Titanium and its Alloy. *International Journal of Science and Research, 3*(10), 1351-1361.
- [5] Sant'Agostino. Impianto in titanio. [online]. Last login: 29 September 2023. Available: <https://www.santagostino.it/it/santagostinopedia/impianto-titanio>
- [6] Kasemo, B., & Gold, J. (1999). Implant surfaces and interface processes. *Advances in dental research, 13*(1), 8-20.
- [7] Kligman, S., Ren, Z., Chung, C. H., Perillo, M. A., Chang, Y. C., Koo, H., ... & Li, C. (2021). The impact of dental implant surface modifications on osseointegration and biofilm formation. *Journal of clinical medicine, 10*(8), 1641.
- [8] Walker, J. (2020). Skeletal system 1: the anatomy and physiology of bones. *Nursing Times, 116*(2), 38-42.
- [9] ROUHI12, G. H. O. L. A. M. R. E. Z. A., & AMANI, M. (2012). A brief introduction into orthopaedic implants: screws, plates, and nails.
- [10] Jin, W., & Chu, P. K. (2019). Orthopedic implants. *Encyclopedia of biomedical engineering, 1*(3), 425-439.
- [11] Zena Dent. Osteointegrazione. [online]. Last login: 30 September 2023. Available: <https://www.zenadent.it/glossario/osteointegrazione/#:~:text=L'impianto%20dentale%20solitamente%20%C3%A8,adatto%20a%20favorire%20l'osteointegrazione>
- [12] Top Doctors. Chirurgia vertebrale: Quali sono i vantaggi per il paziente. [online]. Last login: 30 September 2023. Available: <https://www.topdoctors.it/articoli-medici/chirurgia-vertebrale-quali-sono-i-vantaggi-per-il-paziente>
- [13] Top Doctors. Chirurgia vertebrale: Quali sono i vantaggi per il paziente. [online]. Last login: 30 September 2023. Available: <https://www.topdoctors.it/articoli-medici/chirurgia-vertebrale-quali-sono-i-vantaggi-per-il-paziente>

- [14] Energy Ti. Is Titanium and Titanium Alloy Magnetic? [online]. Last login: 30 September 2023. Available: <https://energy-ti.com/it/is-titanium-and-titanium-alloy-magnetic/>
- [15] Dental Journal. Supplementazione di vitamina D per migliorare l'osteointegrazione. [online]. Last login: 1 October 2023. Available: <https://www.dentaljournal.it/supplementazione-vitamina-d-migliorare-osteointegrazione/>
- [16] GABELLI, G. (2019). Nuova tecnica chirurgica nelle protesi impiantabili per via ossea: risultati preliminari.
- [17] Zena Dent. Osteointegrazione. [online]. Last login: 1 October 2023. Available: <https://www.zenadent.it/glossario/osteointegrazione/#:~:text=L'impianto%20dentale%20solitamente%20%C3%A8,adatto%20a%20favorire%20l'osteointegrazione>
- [18] Verywell Health. Hip Replacement Loosening. [online]. Last login: 1 October 2023. Available: <https://www.verywellhealth.com/hip-replacement-loosening-2548623#:~:text=Hip%20replacements%20usually%20last%20at,hip%20replacement%20to%20come%20loose>
- [19] Archibeck, M. J., Rosenberg, A. G., Berger, R. A., & Silverton, C. D. (2003). Trochanteric osteotomy and fixation during total hip arthroplasty. *J Am Acad Orthop Surg*, 11(3), 163-173.
- [20] Chu, P. K., Chen, J. Y., Wang, L. P., & Huang, N. (2002). Plasma-surface modification of biomaterials. *Mater. Sci. Eng. R Reports*, 36(5-6), 143-206.
- [21] Jemat, A., Ghazali, M. J., Razali, M., & Otsuka, Y. (2015). Surface modifications and their effects on titanium dental implants. *Biomed Res. Int.*, 2015.
- [22] Odekerken, J. C., Welting, T. J., Arts, J. J., Walenkamp, G. H. I. M., & Emans, P. J. (2013). Modern orthopaedic implant coatings—their pro's, con's and evaluation methods. *Modern surface engineering treatments*, 45-73.
- [23] Le Guéhenec, L., Soueidan, A., Layrolle, P., & Amouriq, Y. (2007). Surface treatments of titanium dental implants for rapid osseointegration. *Dent. Mater.*, 23(7), 844-854.
- [24] Albrektsson, T., & Wennerberg, A. (2019). On osseointegration in relation to implant surfaces. *Clin. Implant Dent. Relat. Res.*, 21(S1), 4-7.
- [25] Gill, B. J., & Tucker, R. C. (1986). Plasma spray coating processes. *Materials science and technology*, 2(3), 207-213.
- [26] Mostaghimi, J., Pasandideh-Fard, M., & Chandra, S. (2002). Dynamics of Splat Formation in Plasma Spray Coating Process. *Plasma Chem. Plasma Process.*, 22(1), 59-84.
- [27] Paul, J. P., & Gefen, A. (2003). Optimizing the biomechanical compatibility of orthopedic screws for bone fracture fixation. *Med. Eng. Phys.*, 25(5), 435–436.

- [28] Pulsed Laser Deposition. [online]. Last login: 3 October 2023. Available: <https://www.sciencedirect.com/topics/chemical-engineering/pulsed-laser-deposition>
- [29] Chemical Vapor Deposition. [online]. Last login: 3 October 2023. Available: <https://www.sciencedirect.com/topics/materials-science/chemical-vapor-deposition>
- [30] Deposizione chimica da vapore. [online]. Last login: 3 October 2023. Available: https://it.wikipedia.org/wiki/Deposizione_chimica_da_vapore
- [31] Sol-gel process. [online]. Last login: 3 October 2023. Available: <https://www.sciencedirect.com/topics/chemistry/sol-gel-process>
- [32] Sol-gel process. [online]. Last login: 3 October 2023. Available: https://en.wikipedia.org/wiki/Sol%E2%80%93gel_process
- [33] Scriven, L. E. (1988). Physics and applications of dip coating and spin coating. *MRS Online Proceedings Library (OPL)*, 121, 717.
- [34] Dip coating. [online]. Last login: 3 October 2023. Available: <https://www.apexicindia.com/technologies/dip-coating-technology#:~:text=Dip%20coating%20refers%20to%20the,with%20the%20spin%20coating%20procedure.>
- [35] Cohen, E., & Lightfoot, E. J. (2000). Coating processes. *Kirk-Othmer Encyclopedia of Chemical Technology*, 1-68.
- [36] Marchesa, G. (2021). *Rivestimenti tribologici in TiN depositati tramite tecnologica sputtering per applicazioni innovative sci e snowboard* (Doctoral dissertation, Politecnico di Torino).
- [37] Ensinger Plastics. Industria medica. [online]. Last login: 10 October 2023. Available: <https://www.ensingerplastics.com/it-it/industria-medicale>
- [38] Almeco Group. Trattamento PVD: quanto e quando si può personalizzare? [online]. Last login: 10 October 2023. Available: <https://blog.almecogroup.com/it/trattamento-pvd-quanto-e-quando-si-puo-personalizzare/>
- [39] Sigma Aldrich. Biomedical Materials. [online]. Last login: 10 October 2023. Available: <https://www.sigmaaldrich.com/IT/it/products/materials-science/biomedical-materials>
- [40] Materiale didattico. [online]. Last login: 10 October 2023. Available: <https://www.docenti.unina.it/webdocenti-be/allegati/materiale-didattico/34171555>
- [41] Biochimica applicata. [online]. Last login: 10 October 2023. Available: <http://math.unife.it/lm.biomolecolare/insegnamenti/biochimica-applicata/materiale-didattico/5deg-sds-page-e-isotacoforesi>

- [42] Introduzione generale. [online]. Last login: 10 October 2023. Available: https://moodle2.units.it/pluginfile.php/556293/mod_resource/content/1/3.%20spettroscopia%20infrarossa%20introduzione%20generale.pdf
- [43] Pedrotti, L. S. (2008). Basic physical optics. *Fundamentals of Photonics, 1*, 152-154.
- [44] Sherman Hsu, P. C.-P. (2006). Infrared Spectroscopy Chapter 15. In *Handbook of Instrumental Techniques for Analytical Chemistry* (pp. 607-613).
- [45] Stuart, B. H. (2004). *Infrared spectroscopy: fundamentals and applications*. John Wiley & Sons (pp. 1–248).
- [46] Buijs, H. (2006). Infrared spectroscopy. In *Springer Handbook of Atomic, Molecular, and Optical Physics* (pp. 625-639). Cham: Springer International Publishing.
- [47] Barth, A. (2007). Infrared spectroscopy of proteins. *Biochim. Biophys. Acta - Bioenerg.*, 1767(9), 1073–1101.
- [48] Titanium cranioplasty kit. [online]. Last login: 20 October 2023. Available: https://www.researchgate.net/figure/Titanium-cranioplasty-kit-a-Titanium-plate-b-titanium-mesh-a-b_fig6_51620409
- [49] Niltorg. Spinal Fixation. [online]. Last login: 20 October 2023. Available: <https://www.niltorg.com/info/Spinal-Fixation/MjA=>
- [50] UCSF Orthopedic Surgery. HIP. [online]. Last login: 20 October 2023. Available: <https://orthosurgery.ucsf.edu/sites/default/files/media/documents/04%20HIP.pdf>
- [51] The Journal of Bone & Joint Surgery. Volume 31, Issue 2. [online]. Last login: 20 October 2023. Available: <https://link.springer.com/journal/11639/volumes-and-issues/31-2>
- [52] AAOS. Fracture After Total Hip Replacement. [online]. Last login: 20 October 2023. Available: <https://orthoinfo.aaos.org/en/diseases--conditions/fracture-after-total-hip-replacement/>
- [53] Flamet. Plasma APS. [online]. Last login: 20 October 2023. Available: <https://www.flamet.it/public/index.php/it/processi/processi-a-freddo/plasma-aps>
- [54] Growth of oxide thin films for energy devices by Pulsed Electron Deposition. [online]. Last login: 20 October 2023. Available: https://www.researchgate.net/publication/33436805_Growth_of_oxide_thin_films_for_energy_devices_by_Pulsed_Electron_Deposition
- [55] MKS Instruments. CVD Physics. [online]. Last login: 20 October 2023. Available: <https://www.mks.com/n/cvd-physics>

- [56] Sol-Gel Technology Stages. [online]. Last login: 20 October 2023. Available: <https://upload.wikimedia.org/wikipedia/commons/thumb/5/52/SolGelTechnologyStages.svg/330px-SolGelTechnologyStages.svg.png>
- [57] Spin-coating processes of PCL films. [online]. Last login: 5 November 2023. Available: https://www.researchgate.net/figure/Spin-coating-processes-of-PCL-films_fig1_326537310
- [58] Microbe Notes. Infrared (IR) Spectroscopy. [online]. Last login: 5 November 2023. Available: <https://microbenotes.com/infrared-ir-spectroscopy/>
- [59] Alfatest. Granulometria: i vari metodi di misura. [online]. Last login: 5 November 2023. Available: <https://www.alfatest.it/granulometria-i-vari-metodi-di-misura/#:~:text=La%20setacciatura%20fa%20uso%20di,meccanico%2C%20chiamato%20%E2%80%9Cvibrovaglio%E2%80%9D>
- [60] PerkinElmer. (2011). Ir Ready TOGO (pp. 1–12).
- [61] PerkinElmer. (2017). UNIVERSAL ATR SAMPLING ACCESSORY User's Guide (pp. 1–22).
- [62] PerkinElmer. (2015). SPECTRUM TWO FIXED ANGLE SPECULAR REFLECTANCE ACCESSORY User's Guide (pp. 1–126).
- [63] Freitas, M. V. (2014-2015). Collagene: studio della struttura e delle proprietà [PDF]. Università degli Studi di Pavia. [online]. Available: https://anatcomp.unipv.it/freitas/2014-2015/12_MEC_Collagene_stud.pdf
- [64] Università degli Studi di Trieste. Appunti sulle proprietà dei polimeri (parte 2) [PDF]. [online]. Last login: 20 November 2023. Available: https://moodle2.units.it/pluginfile.php/252854/mod_resource/content/1/Appunti-%20polimeri_introd_2.pdf